MAKERERE UNIVERSITY

RELIABILITY OF STEEL MADE FROM RECYCLED SCRAP IN UGANDA

Candidate: Senfuka Christopher
2008/HD16/4929U

A thesis submitted in fulfillment of the requirements for the award of The Degree of Doctor of Philosophy (Mechanical Engineering) of Makerere University

Year: 2014

DECLARATION

I, Senfuka Christopher, candidate for the degree of Doctor of Philosophy of Makerere University declare that this thesis has not been submitted for a degree in any other University and no Part of the Thesis or Dissertation is plagiarized work.

Candidate: Senfuka Christopher

Sign………………………………… Date…………………………………

Supervisor: Dr. Joseph K. Byaruhanga

Associate Professor

Sign………………………………… Date…………………………………

Co-Supervisor: Dr. John Baptist Kirabira

Associate Professor

Sign………………………………… Date…………………………………

Submitted on:……………………………………………..

Kampala, Uganda

ABSTRACT

While steel can be made from its ores, the industrial world has recognized the advantages of its manufacture through the recycling route especially in view of its economic and environmental friendliness. Steel in Uganda is mainly made through the recycling route. Given the reducing availability of scrap and the growing demand of steel, the quality of the scrap is quickly dropping. In this research, since the usefulness of a material is depicted by its properties, the quality of steel has been studied through the analysis of its mechanical properties namely; ductility, strength, weldability and hardenability. A quantitative experimental research approach has been used along with extensive review of literature. Samples have been selected for examination from the different manufacturers in the country. Attention has been paid to the popular semi-finished product forms like twisted and thermo-mechanically treated (TMT) bars to guarantee the correlation between raw materials input and end use. Samples have therefore been grouped according to product type but have otherwise been randomly selected to eliminate manufacturer identity. A high level of tramp element content has been found consistent in all sample groups. While the bars have been found generally of acceptable ductility, resilience, strength and metallographic properties in spite of relatively high and irregular carbon content, the incidence of fragile samples in each group related to residual element and inclusions content, rolling faults and others has been pointed out. The varying composition in individual steel bars has also been shown to be a factor in the quality of especially the TMT and twisted bars. The wide scatter in yield strength has been found to engender unpredictable concrete reinforcement value. The prevalence of Boron in the range 0.0003% and 0.003% has been shown to play an outstanding role in raising the yield strength and creating development lengths that often exceed the pre-calculated value. Examination of weldments of the bars showed post weld cracks in up to 13% of the samples both in cold and hot cracking. These were also shown to be due to elevated tramp element content rather than carbon content. The incidence uniaxiality of properties also associated to the unpredictable tramp element content was highlighted. On the overall, the use of better sorting methods, more elaborate refining especially at the teeming ladle stage and the exploitation of virgin iron resources to exploit the sponge iron alternative have been recommended. Reducing dependence on Boric acid binding for furnace and ladle lining and chemically reducing Boron content from liquid steel have also been suggested as possible solutions to the unpredictably fluctuating high yield of the steel bars.

Dedicated to my family:

My Wife Patience Birungi

My Children: Joan Nakabira, Rachael Namugenyi, Joel O. Kakande,

Clare Nattabi, Joshua Ggayi and Jemimah Mirembe

For their unchanging love and pride in me

All glory be to the Lord Jesus,

The Christ

ACKNOWLEDGEMENT

This thesis presents the results from the research carried out at Makerere University, Kampala, Kyambogo University and the University of Dar es Salaam.

The largest part of this research has been funded by the Swedish Embassy in Collaboration with the Swedish International Development Agency (Sida) and Makerere University to whom special thanks go for the much needed financial assistance.

I wish to express my sincere appreciation and gratitude to The Directorate of Research and Graduate Training, Makerere University and The School of Graduate Studies, Kyambogo University for their support and offer of this precious opportunity to accomplish my graduate studies. I am very grateful to the Makerere University administration for allowing me carry out my research at this reputable University.

I also wish to express my gratitude to my supervisors: Associate Professor J.K. Byaruhanga and Associate Professor J. B. Kirabira for the professional and personal guidance they have rendered me throughout the extremely demanding times of research tasks.

Recognition goes to members of the technical teams at Makerere and Kyambogo Universities, the secretariat at Gatsby Makerere without whom this accomplishment would have been impossible and the special assistance offered at the University of Dar es Salaam.

Finally, I would like to express my greatest gratitude to my family and friends for their undivided support and for sharing all good and bad moments during the research work. Let me express special gratitude to my parents for their love, support and encouragement throughout my studies.

Special thanks to my wife Patience for the endurance, continuous advice, encouragement and care of our kids during my periods of absence.

Senfuka Christopher

March, 2014

Kampala

TABLE OF CONTENTS

LIST OF FIGURES

LIST OF TABLES

LIST OF PUBLICATIONS

Paper 1: Christopher Senfuka*, John Baptist Kirabira**, Joseph Kadoma Byaruhanga***, Options for Improvement of the Ugandan Iron and Steel Industry. Presented at the Second Interentionl Conference on Advances in Engineering and Tenchnology, Entebbe, Uganda, *Jan. 31st –Feb.1st 2011; 1AET2011 (013).*

Paper 2: Christopher Senfuka*, John Baptist Kirabira**, Joseph Kadoma Byaruhanga***. A Quantitative Evaluation of the Quality of Recycled Steel in Uganda: *A Technical Report*. Presented at the ASME Int. Mechanical Eng. Congress & Exposition, Houston, Texas, USA, *Nov.9th-15th 2012; IMECE2012-85276.*

Paper 3: Christopher Senfuka*, John Baptist Kirabira**, Joseph Kadoma Byaruhanga***. The Concrete Reinforcing Value of Recycled Steel Bars in Uganda. Published in IOSR Journal of Engineering, *ISSN-2250-3021, vol.2, Issue 6, Jan., 2013.*

Paper 4: Christopher Senfuka*, John Baptist Kirabira**, Joseph Kadoma Byaruhanga***. "Weldability of Recycled Steel Bars in Uganda" Published in the International Journal of Engineering and Technology (IJET UK Publications), *ISSN-2049-3444, vol. 2, No.12, Dec., 2012.*

Paper 5: Christopher Senfuka*, John Baptist Kirabira**, Joseph Kadoma Byaruhanga***. Thermo-Mechanically Treated Bars Made from Recycled Steel in Uganda. Published in the International Journal of Engineering and Technology (IJET UK Publications), *ISSN-2049-3444, vol. 3 No. 2, Feb., 2013.*

*Department Of Mechanical And Production Engineering, Faculty Of Engineering, Kyambogo Unviersity, P.O.Box 1, Kyambogo, Kampala, Uganda, *email:* senfukac@gmail.com.

**Deparment of Mechanical Engineering, College of Engineering, Design, Art and Technology, P.O.Box 7062 Kampala, Uganda, email: *jbkirabira@tech.mak.ac.ug*.

*** Deparment of Mechanical Engineering, College of Engineering, Design, Art and Technology, P.O.Box 7062 Kampala, Uganda, email: *gatsby@tech.mak.ac.ug*.

LIST OF ACRONYMS

AISI .... American Iron and Steel Institute

ASM………………………………………….. American Society for Metals

ASME……………………………………… American Society of Mechanical Engineers

BIR………………………………………….. Bureau of International Recycling

CRM………………………………………….. Centre for Research in Metallurgy

DOI………………………………………… Department of Interior, USA

DRI ……………………………………………Direct Reduced Iron

EAS……………………………………………East African Standard

HBI……………………………………………Hot Briquetted Iron

EAF……………………………………………Electric arc Furnace

Eurofer…………………………………….. European Confederation of Iron and Steel Industries

HAZ……………………………………….. Heat Affected Zone

HB……………………………………………Hardness Brinnel

IF………………………………………………Induction Furnace

ISO……………………………………………International Organization for Standardization

MARTEC …………………………………..Maritime Technologies

MMA ………………………………………..Manual Metal Arc

TMT………………………………………... Thermo-Mechanically Treated Bars

UBOS ……………………………………… Uganda Bureau of Statistics

URA………………………………………. Uganda Revenue Authority

CHAPTER ONE: INTRODUCTION

1.1 Background

Steel has played a significant role in the world economic development. The main reasons for its popularity have been its relatively low cost of making, forming, welding and processing, the abundance of its two raw materials namely; iron ore and scrap, and its unparalleled range of mechanical properties. There are over 2500 steel grades either published, registered or standardized worldwide, all of which have different chemical compositions although up to 90% of the world steel production falls in the plain carbon range (Vogel *et al,*2006*)*. In addition, all the different possible heat treatments, microstructures, cold-forming conditions, shapes, and surface finishes mean that there is a huge number of options available to the steel user.

One of the most positive aspects of steel, however, is its ease and limitlessness of recycling repeatedly without substantial degradation in quality when steel products reach the end of their designated lives.

In recycling, products at the end of their designated service lives and otherwise only fit for the landfill are re-melted into fresh raw material. The ability to recover and collect old steel products for subsequent re-melting is greatly enhanced by the inherent magnetic properties of steel and consequently, a large tonnage of steel becomes available for recycling every year.

History has shown, however, that scrap availability is never sufficient to meet global demand for new steel. In Figure 1.1, it can be seen that although the tonnage of steel recycled globally is rising, the level of recycled content which is sometimes used as an indicator of resource efficiency, is actually diminishing (Chatterjee, 1995).

Steel scrap occurs in three major varieties:

a) Home scrap (plant scrap) generated in the steel mills during the steel production process. This is relatively pure and its composition known;
b) Process scrap (prompt scrap) generated in the process of manufacturing industrial and consumer end steel products and;
c) Obsolete scrap (Post consumer scrap) which consists of iron and steel products discarded after the end of their service life.

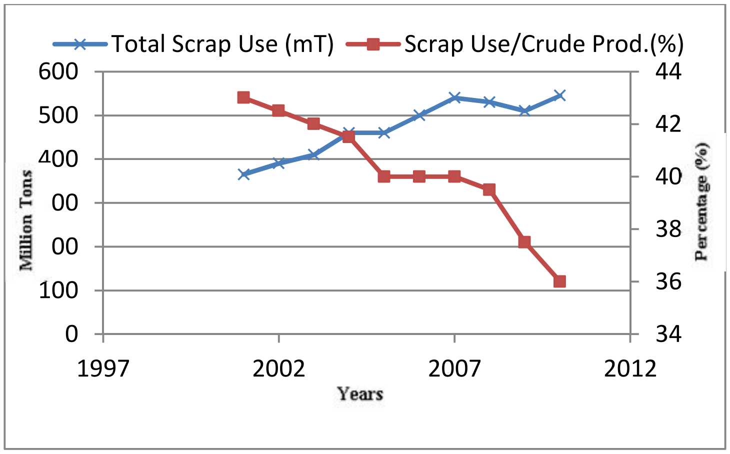

Fig 1.1: Dropping Global Scrap Availability (BIR, 2011)

At least 50% of all scrap is in the obsolete group and is often mixed, coated or in chemical combination with other materials such as zinc, copper, tin, glass, plastics etc. These are the major sources of tramp or residual elements in steel.

Any contaminant in a casting or component's chemical composition whose presence is unimportant or undesirable to the quality of the casting and whose removal though viable industrial economical metallurgical processes is not practicable is called a tramp or residual element (Janke, *et al*. 2000). The tramp element content of steel is usually at trace levels and has a widely fluctuating chemical composition depending on its origin and degree of prior recycling. For practical purposes, all scrap will be considered of the obsolete variety.

The occurrence of obsolete scrap depends on previous manufacturing and numbers of end-of-life steel products. This is a largely challenging position for the developing world, for while in Germany, for example, on the average 70% of the tonnage of steel end products is returned into the materials cycle 20 years after the manufacturing (Janke *et al*., 2000), the conditions of collection and consumption of obsolete scrap in developing countries definitely make it impossible to obtain even a fraction of such levels of recycling although the steel production in these countries is increasingly dependent on scrap.

The Ugandan iron and steel industry has been growing at unprecedented rates averaging from 20% and 30% per annum for imports and exports respectively between 2002 and 2006 due to the booming housing and construction sector in the region (URA, 2010). Steel made from recycled scrap is almost entirely used for building and construction industry in its concrete reinforcement or plain bar form (Oliver *et al*, 2006).

The steel industry is donned with a few companies which have been operating steel mills in the country over the years, first based on imported billets and later predominantly using scrap iron. From the 1960s to 1988, the Madhivani run East African Steel Corporation in Jinja carried out steel production. Steel Rolling Mills under the Alam Group of companies was also established at Jinja in 1987. BM Technical Services in Mbarara run by local entrepreneurship also began operations while more recently in 2002, Tembo Steel Mills was added to the list followed by Modern Steel International Ltd and Pramukh Steel Ltd in Njeru, Jinja and much later in 2010 by Roofings Steel Rolling Mills and Tiang Tang Steel Rolling Mills both in Mukono District. These industries have enabled substantial import substitution, supporting the rapidly expanding building and construction sector and are the major reason why the ratio of the imported steel products to the exported ones has generally been reducing (Fig. 1.2).

Relying basically on scrap, these mills currently suffer from a shortage of raw material. Globally, scrap constitutes at least 70% of mini steel mills input (Janke *et al*, 2000). This shortage has negatively affected the quality of their products and led to fervent competition among them for scrap input, making their continued existence quite doubtful unless something changes soon.

In order to make the recycling process possible, obsolete steel components are purchased, sorted and melted either in induction or arc furnaces through a process in which the composition of the resulting steel is controlled using decarburizers, deoxidizers and alloying additives.

The liquid steel is then cast into billets and cut into blooms of required lengths before being left to cool in still air. These are then taken to reheating furnaces mainly of the oil fired pusher type and either rolled into thermo-mechanically treated (TMT) bars or made into bars which are either twisted into reinforcement bars or used for fabrication of welded products and other structures.

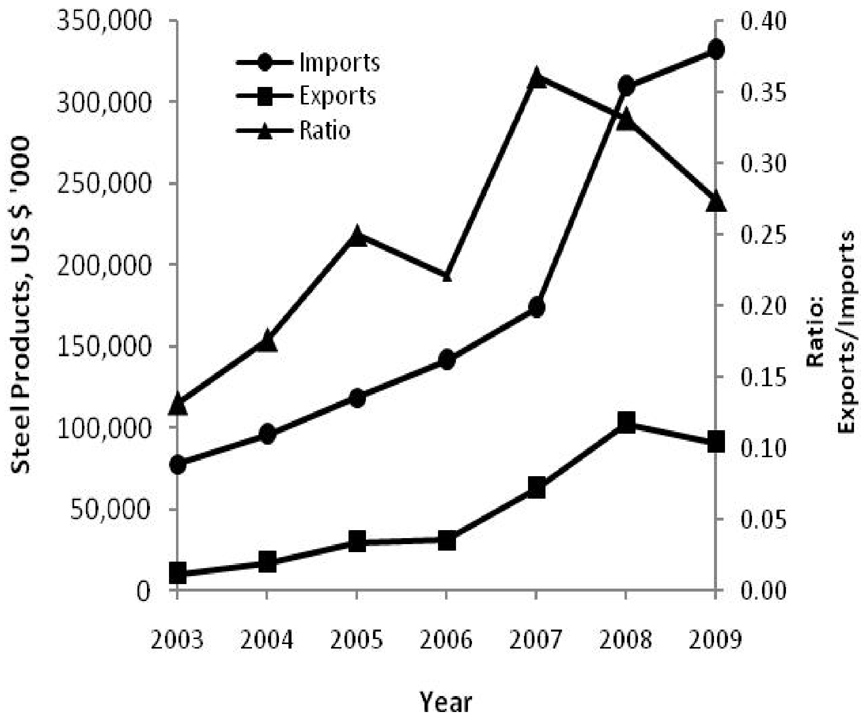

Fig 1.2: Exports and Imports trends in Ugandan Steel Industry (UBOS, 2009)

In spite of the dependence of the quickly growing building and construction industry on steel manufacturing as well as the expanding investor interest in the field, little has been done to keep a keen track of the quality of steel.

1.2 Problem Statement

Due to shortage of good quality steel scrap in the county, recycled steel manufacturers tend to melt all kinds of stock whose variability in composition makes it hard to guarantee the quality and consistency of steel got from them. Fig.1.3 shows a typical lorry load of scrap at Kisenyi in Kampala destined for a steel factory in Jinja. Iron sheets are a source of zinc while utensils are basically stainless steel.

This has often led to:

i) Steel bars failing frequently on bending and on welding.

ii) Different parts of the same bar of the bar behaving differently when subjected to the same conditions while bars from the same batch are even more varied.

In Fig. 1.4(a), a steel bar in the construction industry could not be bent though ninety degrees without fracture while in 1.4(b), a welded joint tears in the parent metal.

There is therefore need to investigate the source and extent of these short comings, quantify them and suggest a way forward based on reliable scientific information.

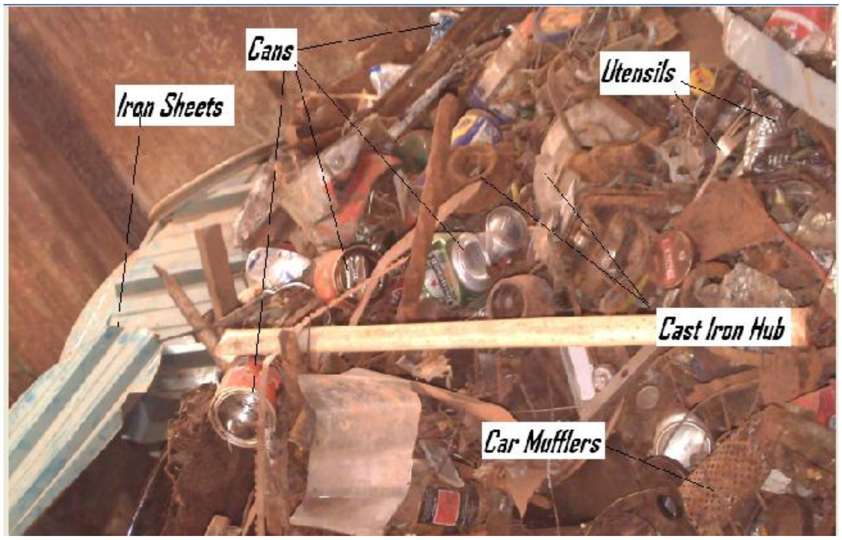

Fig 1. 3: Scrap collection at Kisenyi, Kampala destined for Jinja

Fig. 1.4(a): Square bar cracks on

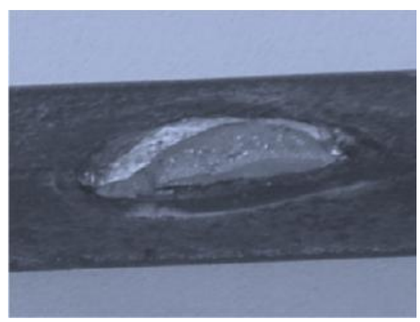

Fig. 1.4(b): Failure of weld in parent metal

1.3 Objectives

1.3.1 Main objective

The major objective of the study was to investigate the reliability of steel made from recycled scrap in Uganda.

1.3.2 Specific objectives

a) To determine the current state of steel industry in Uganda.

b) To determine the general mechanical properties of the steel made from scrap in Uganda.

c) To determine the suitability of the strength and ductility of recycled steel in Uganda for concrete reinforcement.

d) To determine the suitability of the weldability of recycled steel made in Uganda for welding/fabrication applications.

e) To determine the suitability of the hardenability of recycled steel made in Uganda for reinforcement bars.

1.4 Justification

Steel production and consumption is an accepted yardstick for the level of industrial development in any country. The quality of steel is therefore an integral part of all national development.

There is wide spread use of recycled steel products nationally and internationally. The quality of these products, however, is constantly varying and has been taken for granted. This quality needs to be established and quantified since currently almost all building construction and structural engineering in the country rely on the steel and hence human lives are at stake. Recycled steel is more prone to chemical, mechanical and other pedigree based faults than any other iron and so the identification of recurrent deficiencies is paramount in order to correctly allocate zones of safe deployment and also highlight avenues to improving on the outstanding shortcomings.

1.5 Conceptual Framework

The processes were started by the collection of samples followed by chemical and physical analysis. The properties were then determined from the data analysis leading to the determination the quality of the steel made from scrap. All visits were made in order to observe processes and quality control.

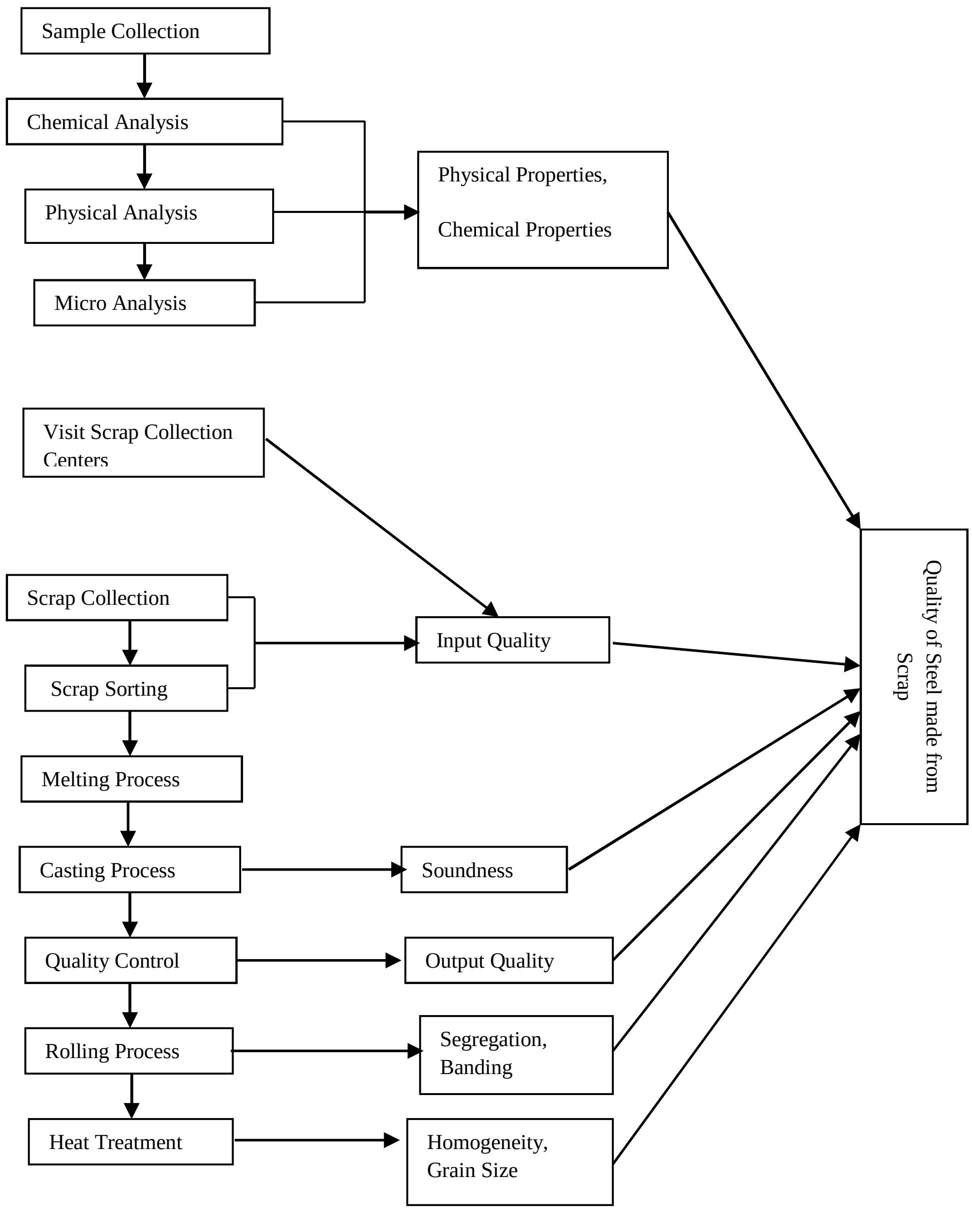

Fig.14: Conceptual Framework

1.5 Scope

The research concentrated on the quality of steel made from ferrous scrap in Uganda paying particular attention to the manufacturers currently in place, their inputs, equipment, product quality and their suitability for the required applications.

1.6 Research Questions

a) What is the current state of steel industry in Uganda?

b) How do the mechanical properties of the steel made from scrap in Uganda compare with the standard values?

c) How suitable are the strength and ductility of recycled steel in Uganda for application in concrete reinforcement?

d) What is the suitability of the weldability of recycled steel made in Uganda for welding/fabrication applications?

e) How suitable is the hardenability of recycled steel made in Uganda for reinforcement bars application?

1.7 Outline of the Thesis

This thesis deals with the quality of steel made from scrap in Uganda and has been divided into the following papers and summary:

Paper 1: "Options for Improvement of the Ugandan Iron and Steel Industry" Christopher Senfuka[*], John Baptist Kirabira[**], Joseph Kadoma Byaruhanga[***] to address the first objective.

Paper 2: "A Quantitative Evaluation of the Quality of Recycled Steel in Uganda, *A Technical Report*" Christopher Senfuka[*], John Baptist Kirabira[**], Joseph Kadoma Byaruhanga[***] to address the second objective.

Paper 3: “The Concrete Reinforcing Value of Recycled Steel Bars in Uganda”, Christopher Senfuka[*], John Baptist Kirabira[**], Joseph Kadoma Byaruhanga[***] to address the third objective.

Paper 4: “Weldability of Recycled Steel Bars in Uganda” Christopher Senfuka[*], John Baptist Kirabira[**], Joseph Kadoma Byaruhanga[***] to address the forth objective.

Paper 5: “Thermo-Mechanically Treated Bars Made from Recycled Steel in Uganda” Christopher Senfuka[*], John Baptist Kirabira[**], Joseph Kadoma Byaruhanga[***] to address the fifth objective.

*Department Of Mechanical And Production Engineering, Faculty Of Engineering, Kyambogo Unviersity, P.O.Box 1, Kyambogo, Kampala, Uganda, *email:* *senfukac@gmail.com*.

**Deparment of Mechanical Engineering, College of Engineering, Disign, Art and Technology, P.O.Box 7062 Kampala, Uganda, email: *jbkirabira@tech.mak.ac.ug*.

*** Deparment of Mechanical Engineering, College of Engineering, Disign, Art and Technology, P.O.Box 7062 Kampala, Uganda, email: *gatby@tech.mak.ac.ug*.

The first paper is about the ‘state of the art’ of the Ugandan steel industry. It sets out to look at the state of the iron and steel industry in Uganda, comparing and contrasting the local position with that of other steel producers worldwide, highlighting ways to improve the production processes and quality of the steel. This was done by considering the existing resources and the possibility of their reinforcement using viable modern scientific methods of exploitation as justified by current production and market development trends. The prominence of the small and medium scale producers in the field, the effect of the scrap as major input and quality related issues were reviewed. The importance of scrap cleaning and virgin ore availability and exploitation were also discussed.

The second paper evaluates and relates the chemical, mechanical, metallurgical and geometrical properties of locally made steel bars commonly destined for building and structural fabrication purposes in order to identify the factors underlying the performance of the products made from them and examine the relationship with their scrap content. The geometrical consistency of the bars was also examined.

The third paper investigates the relationship between the elevated yield values highlighted in Paper 2 and the residual element content which in turn is a direct result of steel recycling. It emphasizes the connection between the ductility of the hot rolled reinforcement bars made from this steel and the tramp element content in them, examining the relationship between the relatively high tensile strength, the corresponding yield strength and ductility and their capacity to fulfill their role as concrete reinforcing twisted bars.

The forth Paper hinges on the weldability of the bars made from recycled steel in Uganda and analyzes the consequences of their recycled content and the resulting residual element content. An analysis of the soundness of the manual arc welds is made focusing on the incidence longitudinal and transverse hot and cold weld crack formation and the frequent occurrence of inclusions, minor phase particles, microscopic cracks, and other discontinuities in bars of less than 0.3% carbon content.

The fifth paper, looking at thermo-mechanically treated bars made from recycled steel in Uganda is a study of the hardenability values of the steel. The recycled origin of these steels, which gives rise to the abundance of residual elements, has been related to the effect of these elements on the quality of the locally made TMT steel bars since the alloy (tramp) element content is the major factor in determining the hardenability of steel which in turn give the hardness distribution pattern in the steel bar section in order to examine their suitability for the building industry.

CHAPTER TWO: REVIEW OF LITERATURE

2.1 Steel Making

Two basic modes of steel making are used worldwide; the primary and secondary processes. The primary steel manufacturing process comprises iron making in which iron ore is converted into liquid iron (pig iron) followed by steelmaking in which the pig iron is made into steel, casting during which liquid steel is made to solidify into ingots or billets depending on the casting process, billet rolling in which the blocks are reduced to steel bars and product rolling involving the making of finished or near finished shapes. All these stages are carried out successively in a typical integrated mill (Jung *et al*, 2005).

The principal raw materials for an integrated mill are iron ore, limestone and coal (or coke). These materials are charged in batches into a blast furnace where the iron compounds, mainly heametite (Fe_2O_3) and magnetite (Fe_3O_4) in the ore give up oxygen in the presence of carbon from the coal and become liquid iron. At intervals of a few hours, the accumulated liquid iron is tapped from the blast furnace and either cast into pig iron or directed to other vessels for further steelmaking operations (Tupkary *et al*, 2008).

Commercial bulk steel production began with the invention of the Bessemer process in the mid-19th century. The key principle was the removal of impurities from pig iron by oxidation with air blown through the molten iron. During the process, impurities such as silicon, manganese and carbon were removed in the form of oxides which either escaped as gas or formed slag. The oxidation also raised the temperature of the iron mass and kept it molten. The Bessemer process was so fast (10–20 minutes for a 15 to 20 ton heat) that it allowed little time for chemical analysis or adjustment of the alloying elements in the steel (Madar, 2009). Bessemer converters therefore did not remove phosphorus efficiently from the molten steel and the nitrogen from the air made Bessemer steel inherently fragile while the process thermal efficiency was affected by the non-reactive nitrogen in air blast.

The basic oxygen steelmaking, a primary process in which the carbon-rich molten pig iron is made into steel by blowing oxygen instead of air through molten pig iron soon replaced it. This was carried out in basic calcium oxide and magnesium oxide refractory lined furnaces to lower the carbon content of the alloy and change it into low-carbon steel.

Secondary steel processing, the major steel production mode in Uganda, is usually carried out in mini-mills and obtains most of its iron from scrap steel recycled from used equipment or byproducts of manufacturing. Direct reduced iron (DRI) is sometimes used with scrap to help maintain the desired chemistry of the steel (Ibrahim, 2010). The necessary processing of DRI from the mineral ore is still at infant stages in Uganda. The steel processing is done in electric furnaces being either of the arc or induction type. A typical mini-mill in Uganda will thus have an electric arc or induction furnace for scrap melting, a ladle furnace to administer liquid metal and control its pouring temperature, a billet continuous caster for converting molten steel to solid form, a reheat furnace and a rolling mill. Some of the steel mills however still feature non-continuous ingot casting facilities.

2.1.1 The electric arc furnace

In the electric arc furnace (EAF), the steel making temperature is obtained using an arc, struck between three carbon electrodes fed from a three phase supply input and the metallic charge housed in a basic lined shell. Traditionally, this was run on cold charge. A more modern inclination, however, is to introduce hot metal as part of the scrap input. The power needed to melt the charge ranges from 600kwh/t for small and medium size furnaces popularly used in the country to 450kwh/t in big furnaces while between 150 and 400kwh/t is needed for refining (Beno *et al*, 2013).

The EAF process incorporates refining details. Refining operations in the electric arc furnace have traditionally involved the removal of phosphorus, sulfur, aluminum, silicon, manganese and carbon from the steel after melt down and are all dependent on the availability of oxygen. Oxygen is lanced at the end of meltdown (Ibrahim, 2010). Since most of the compounds to be removed during refining have a higher affinity for oxygen than carbon, oxygen preferentially reacts with these elements to form oxides which float out of the steel into the slag. Iron ore is added to the boil to start the oxidation of carbon, leading to the production of carbon monoxide (CO). This CO evolved within the steel bath helps to remove nitrogen and hydrogen from the steel. Bath samples are periodically taken out for quality control. Lime and spur are added to impose the slag shape.

2.1.2 The induction furnace

All steel making plants in Uganda currently use induction furnaces to melt steel scrap into long steel semi-finished products to some extent. Fig.2.1 shows the configuration of a typical crucible used in a local induction furnace while in Fig. 2.2, the overall process is represented in a flow chart. In this steel mill in particular, two 8 ton furnaces work simultaneously to produce 150 tons of steel per day of two shifts. Four crucibles are arranged to work two at a go, one for each furnace while the other pair is relined.

The relining process consists of inserting of a mild steel former in the center of an opening in the platform and winding around it, 6mm copper tubing inside which an asbestos ring inserted (Fig. 2.1).

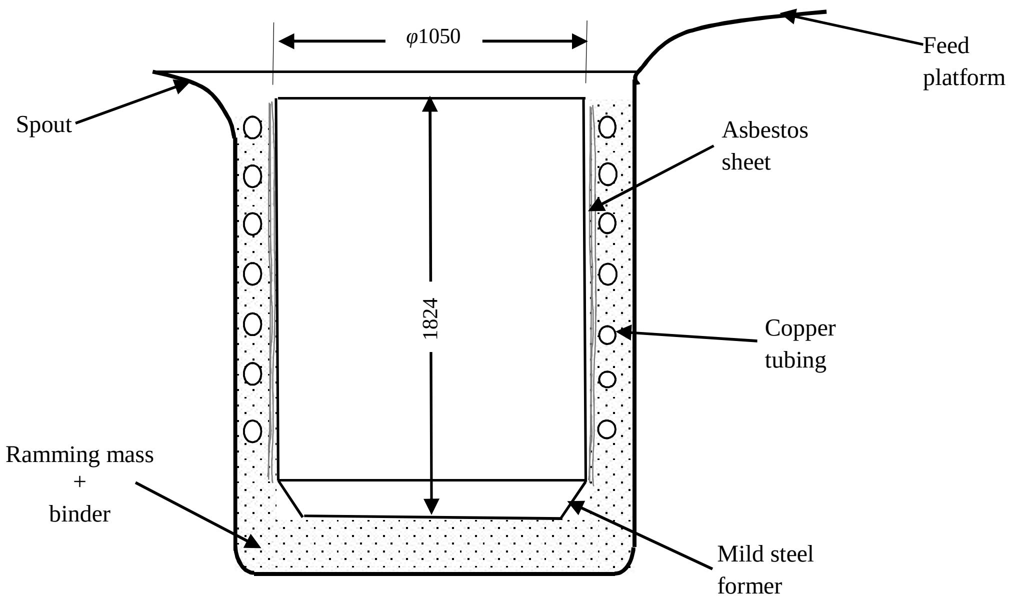

Fig 2.1: Re-lining the Induction Furnace

Mica insulators are also placed between coils to discourage short circuiting between them. The remaining space is filled with a magnesite ramming mass fixed with boric acid binder. The lining is finally sintered by passing current for 3 hrs, a process which also removes moisture.

Scrap, delivered in trucks, is sorted first manually and then electro-magnetically. Light scrap is compacted with the help of a baling hydraulic press. The entire scrap load is then delivered to the feed platform (Fig 2.1) and fed into the furnace crucible, light scrap first, before the melting process is started.

The induction furnace, set at 480 to 540Hz takes 2½ to 3hrs to melt the 8 ton crucible, heating it to 3500°C. Samples are taken when the liquid steel level reaches ¼, ½, ¾ and full capacity of the furnace for quality control. The carbon content is managed using mainly ferric oxide (equation 2.1) from mill-scale derived from the rolling process since iron ore additions tend to agitate the steel bath excessively, leading to boiling over.

$$2Fe_xO_y + yC \rightarrow 2xFe + yCO_2 \ldots\ldots\ldots\ldots\ldots\ldots 2.1$$

Slag is poured off into the slag pot and constitutes about 20% of the molten material and 50kg of manganese silicon added. Ferrous silicate follows. The subsequent reactions raise the temperature of the melt high and the addition of 5kg pieces of aluminium helps control the bath temperature and finalize deoxidation prior to pouring of the melt into the waiting dolomite lined ladle.

The 20 ton capacity ladle, carried by the overhead crane, takes the contents of the two furnaces to the continuous caster. Its sliding dispenser is worked by a hydraulic opener to release the liquid steel into the tundish whose level is maintained constant in order to keep a stable head by controlling the ladle opening. The tundush has two openings which serve two moulds at a go, thus casting two billets. The mould oscillates inside the water cooled mould jacket (primary cooling) at 30 to 60 cycles per minute with a stroke of 12 to 40 mm depending on the rate of withdrawal in order to guarantee a negative strip pattern. This is in order to discourage friction, sticking and crack formation in the solidifying shell and minimize liquid steel breakouts while a strong water spray cools the copper mould which in turn gives the billet cross section its shape (Fig. 2.3). Mould lubrication oil is also used to curtail friction.

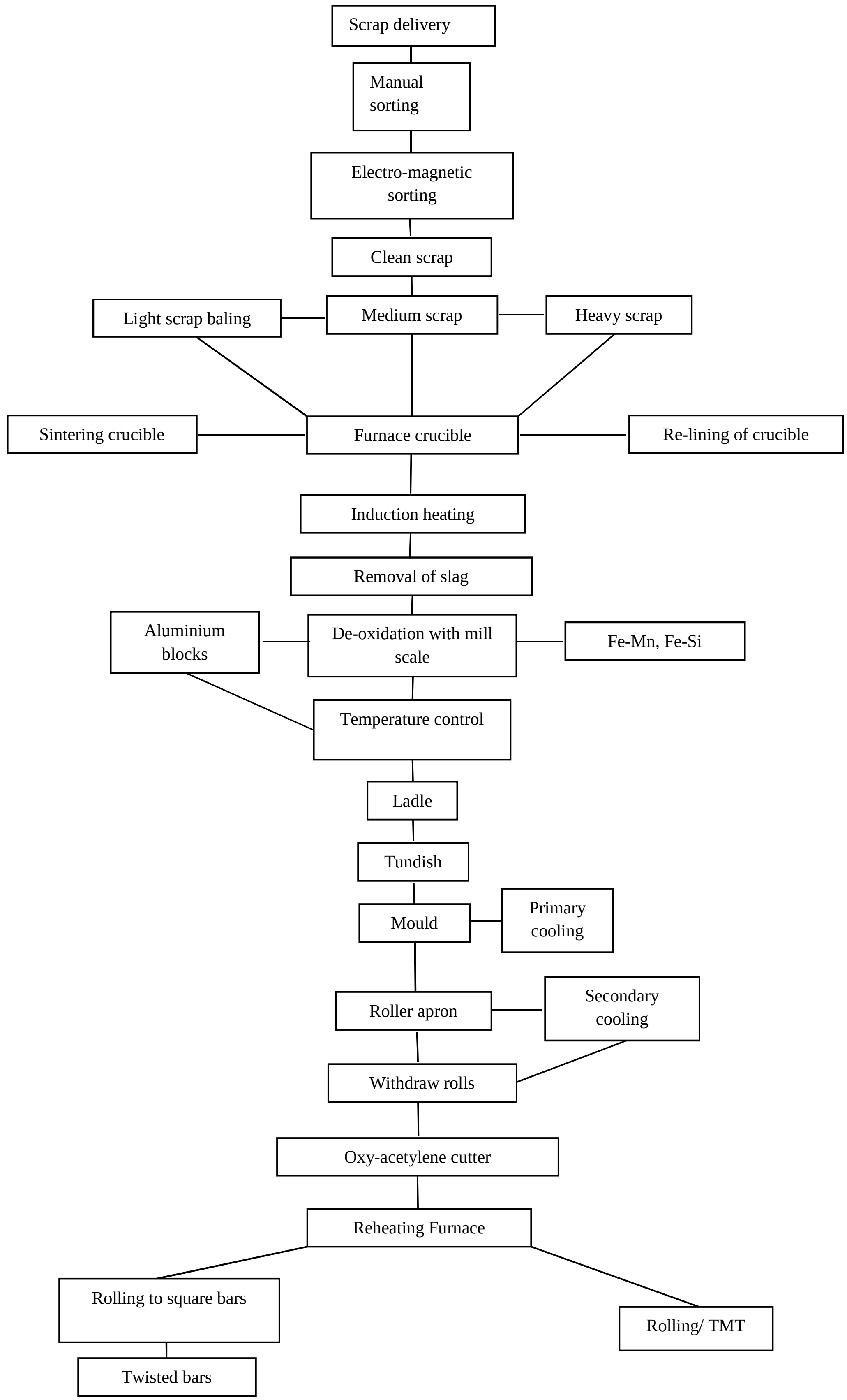

Fig 2. 1: Flow Chart of Induction Furnace Steel Making

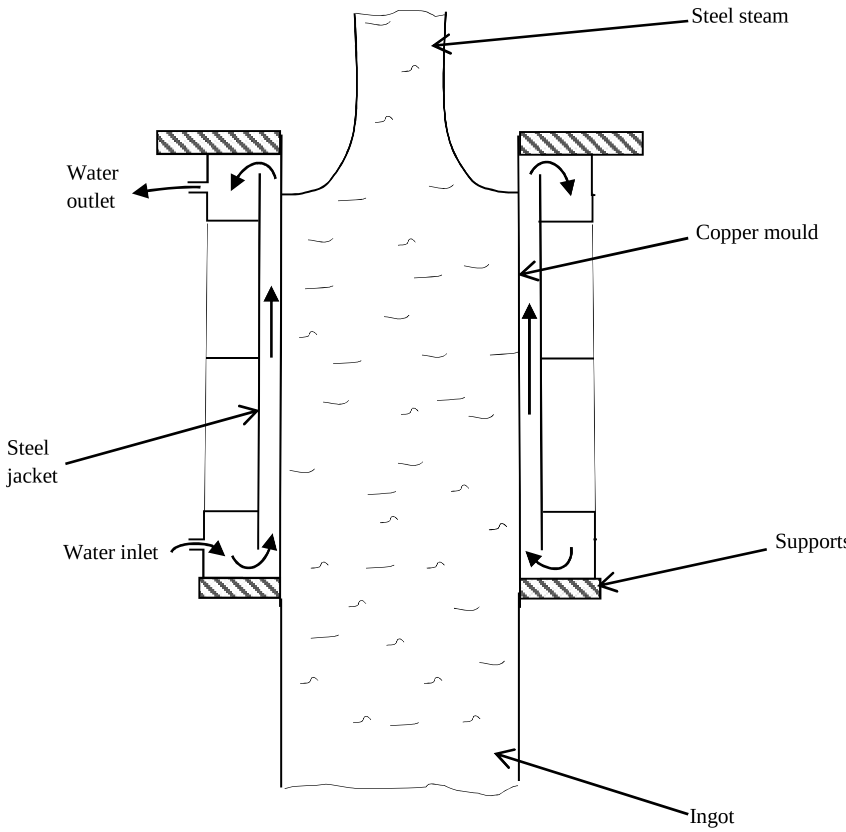

Fig 2.2: Mould of Continuous Casting Machine

Having accomplished the initial (primary) cooling in the mould and formed the solid outer billet shell, solidification of the core and further temperature reduction is achieved using high pressure water sprays (secondary cooling). The roller apron helps shape and guide the billet while the withdraw rolls give it the required travel rate and determine the product temperature profile (Fig.2.4). The final output, a 100mm square section is pulled at about 3m/min by the withdrawal rolls. The billet is later cut using an oxy-acetylene gas cutter to convenient economic lengths in accordance to the intended final bar size which are sent to the cooling beds where they are kept pending reheating in the reheating furnaces prior to being rolled. The reheated bars at 1100°C are then rolled into thermo-mechanically treated (TMT) or square bars for direct use or later forming into twisted bars.

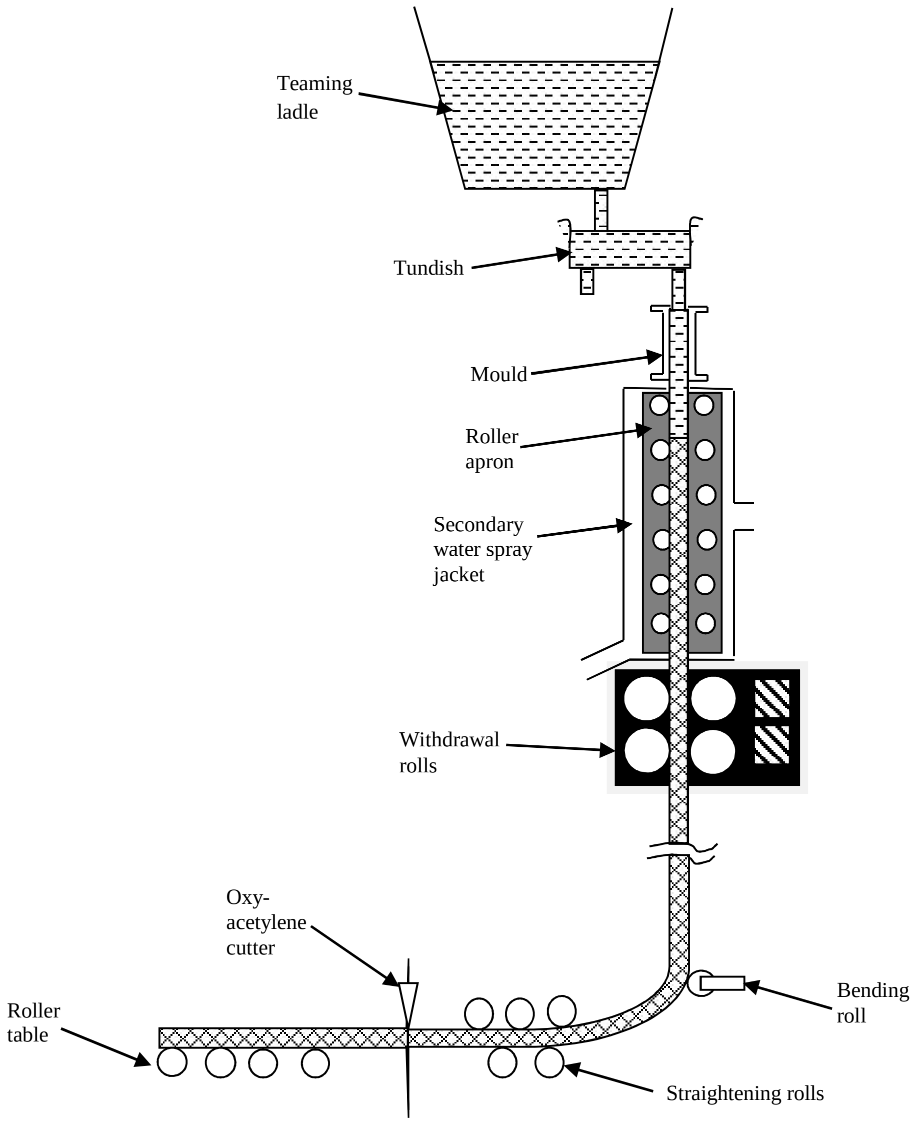

Fig 2.3: Arrangement of Continuous Casting Machine

2.1.2.1 Induction furnace with sponge iron

With the reducing scrap availability and growing induction furnace numbers in the country, the quality of scrap has become a major issue and has necessitated the search for an alternative raw material. The problem has been tackled by reverting to sponge iron (also called direct reduced iron, DRI) which not only provides a possible substitute for scrap but also turns out to be more suitable melting stock for the production of good quality steel. DRI is characterized by uniform chemical and physical characteristics, hardly contains any tramp metallic elements (being about 0.02%) and is low in sulphur content (0.012 to 0.015% S). It also has a high degree of metallization which varies from 85 to 95% depending on the process adopted for its production (Valipour , 2009).

In making DRI, iron ore is reduced in solid state at 800 to 1,050^{o}C either by using reducing (natural) gas (H_2+CO) or coal. Direct reduced iron can be produced in lumps or pellets. Selected proportions of lumps and pellets with high iron content, low gangue content, good mechanical strength that are readily reducible and of non-decrepitating variety are hot pressed at 700^{o} to 800^{o} C immediately after the reduction of the ore and are used to make hot briquetted iron (HBI) (Grobler *et al*,1999). HBI has a higher density and lower specific surface area which improves the resistance to reoxidation and makes it easier to handle than sponge iron. (Wolfgang, 2006).

The oxygen in the DRI present in the form of FeO reacts vigorously with carbon in the molten bath, fostering improved heat transfer, slag-metal contact and homogeneity of the bath. Carbon is thus required and that is why gas based DRI with carbon content 1.0 to 2.5% C is better steel making material than of coal based DRI with only an average 0.2% C (Dutta, 2004).

For induction furnace melting purposes, the gangue and unreduced iron oxide content of DRI should also be maintained as low as possible for safety reasons as well as for energy consumption reasons. Large quantities of unreduced iron oxide in the high carbon bath at high temperatures causes vigorous carbon boil that could be extremely dangerous (Arabinda *et al*, 2011). An induction furnace for melting DRI should be constructed with a large ratio of cross sectional area to volume to enhance heat transfer in order to keep the slag hot and fluid (Dutta, 2004).

By using DRI, the residual element content is remarkably reduced (Fig.2.5) in steel so that the highest quality products can be made with excellent formability and aging characteristics.

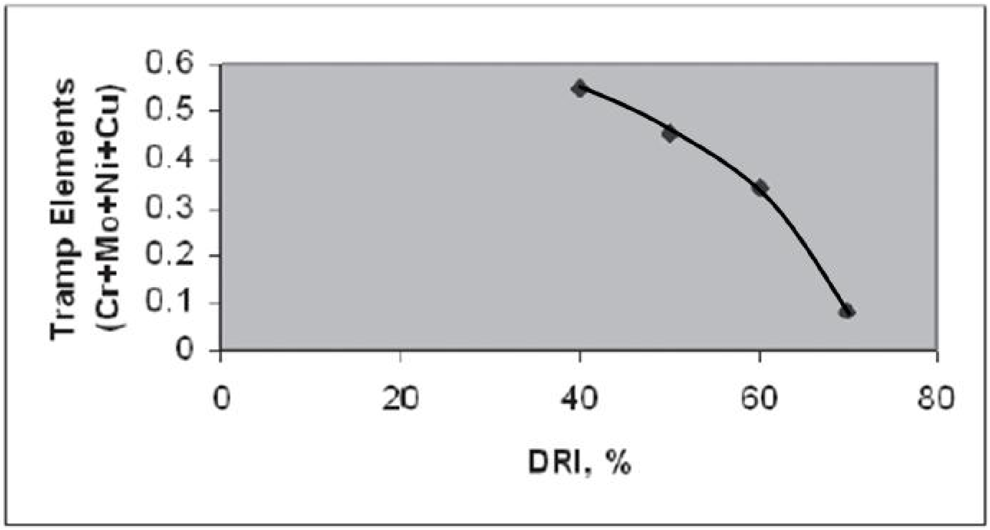

Fig 2. 4: Effect of DRI charge on steel tramp element content (Dutta, 2004).

2.2 Steel Composition

Plain carbon steel consists of mainly iron and carbon. In any given type of steel, however, there is always a certain amount of other elements some of which are added intentionally as alloy elements while others, so called residual or tramp elements, are carried over from prior processing or raw material which is mainly scrap in this case.

2.2.1 Deleterious tramp elements

Most reinforcement bars are made of recycled steel worldwide either through the electric arc or induction furnace process (BIR, 2011). Research has, however shown that owing to the tramp element content, recycled steel is more prone to certain defects than steel from the primary steel production process. For instance it is believed that micro-cracks form during continuous casting or hot forming that are not eliminated during subsequent processing and cause surface defects resulting in surface hot shortness in final product and secondly, that steel slab surface cracking in the continuous casting process is affected by hot ductility of steel in the austenite to ferrite transformation temperature range (O’Neill, 2002). The low hot ductility in the reheating temperature range, 600-950°C, in some low carbon and low alloy steels is a serious industrial problem. Tin and copper are the critical elements here (Olivier *et al*, 2006). The allowable maximum copper content varies widely between 0.15% and 0.5% depending on the type of steel, degree of hot working and cold working used in converting steel into usable forms and the amount of other impurities present, especially Tin, known to have an intensifying effect on Copper quantifiable as in

$$\%Cu + 8 \times \%Sn \leq 0.45 \quad \ldots\ldots\ldots\ldots\ldots\ldots\ldots\ldots 2.2 \text{ (ECP, 1993).}$$

Melford in his publication 'The Influence of Residual and Trace Elements on Hot Shortness and High Temperature Embrittlement' published in 1980 with The Royal Society, had earlier talked of how bulk hot brittleness in which residual elements, by giving rise to the formation of second phases, impede the grain boundary mobility and recrystallization of austenite during deformation and initiate fracture without even the formation of any liquid intergranular films.

Anxiety about the quality of steel made from scrap is therefore not new. Uchino *et al*, 2001 in their paper 'Effects of C and P on surface hot shortness of steel due to Cu mixed from steel scrap' also argue that when scrap iron is recycled, surface cracks occur during the steel hot rolling process. They attributed this phenomenon to Cu accumulated from continual recycling and being enriched at the steel-scale interface by the selective (preferential) oxidation of iron above 1083^0C. They argue that the austenite grains are penetrated by the then liquid (copper) phase and that this results in surface cracks which are ultimately sources of serious cracks even after cooling. This often occurs with copper contents over (0.1 – 0.2) % (Yamamoto *et al*. 2005).

Nevertheless, Fujda Martin, in his article "Effect of Copper Content on the Hot Ductility Loss of Low Carbon Steels" published in 2003 contends in his study of low carbon steels with copper contents 0.04%, 0.38% and 0.63% done at the $\gamma \rightarrow \alpha$ transformation temperature range, that the highest ductility loss is predominantly caused by the formation of pre-eutectoid ferrite along the austenite grain boundaries and that this results in crack formation and the coalescence of micro-voids in the pro-eutectoid ferrite located at the $\gamma \rightarrow \alpha$ interface and that, since the flow stress of the pro-eutectoid ferrite is significantly lower than that of the austenite grains at this temperature, plastic deformation occurs preferentially in this ferrite, leading to crack or void formation (Fig. 2.6).

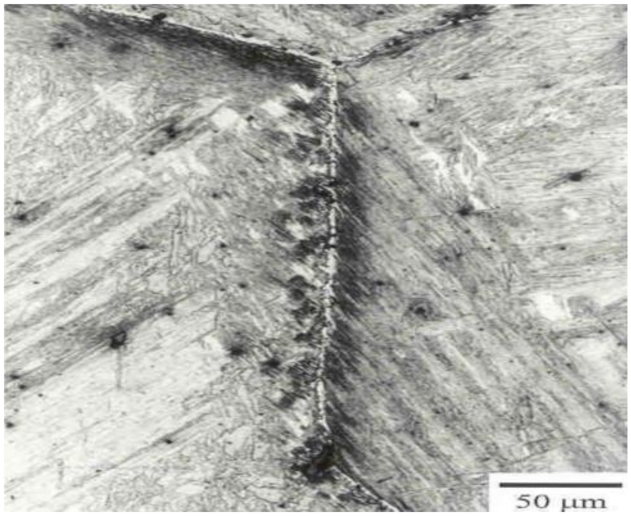

Fig 2. 5: Film-like Proeutectoid Ferrite (Fijda, 2003)

Other residual elements impose complex modifications on the hot shortness caused by copper. Although many of the early investigations considered the influence of individual trace elements on hot ductility, in practice such relatively simple situations seldom arise. More often than not it is the interaction between a combination of trace elements which has to be understood if their net influence on high temperature mechanical properties is to be evaluated (Melford, 1980). Several studies refer to the copper equivalent. Nylén (1982) reports copper equivalent as:

$$Cu_{equ} = \%Cu + \frac{1}{n}\left[0.4(5Mn + \%Cr) + 8(\%Sn + \%Sb) + 2\%As - \%Ni\right] \leq A ....(2.3)$$

where n is the number of elements in the equation and A is a value depending on experimental and production parameters and on the type of steel.

More importantly, in the equation above, the elements which have the strongest influence on Copper hot-shortness are Tin and Antimony. The combination of Tin and Copper greatly increases the susceptibility to hot-shortness of steel. Tin lowers the melting point of the copper phase and decreases the solubility of copper in iron causing further enrichment of this phase.

On the other side, Nickel increases the solubility of Copper in austenite and raises the melting point of the Copper enriched phase, lessening its susceptibility to hot-shortness.

Further research has also shown that, the addition of Cobalt, Nickel and Aluminium results in an increase of the solubility of Copper, while that of Vanadium, Chromium, Manganese, Silicon and Tin decreases copper solubility. Increasing the solubility of Copper should decrease hot-shortness as less copper would build liquid films at the austenite grain surface (Othani *et al*; 1997).

The hot ductility of low carbon steels ($\approx$0.15%C) containing Tin was found to decrease with increasing Tin content and is least at 750^{0}C. Non-equilibrium grain-boundary segregation of Tin produced during cooling is primarily responsible for the decrease in the hot ductility of the steel containing Tin, the critical cooling rate for the tin segregation was located between 5 and 20 ^{o}K/s. (Yuan *et al*, 2003).

The microstructure after hot-working has a direct effect on the mechanical properties of the steel and its behavior during cold working (Olivier *et al*, 2006). Among the material properties desired to favor subsequent cold working operations are good elongation and drawability. The drawability of the material is quantified by the r-value, the quota between the contraction of the material in the width direction and the contraction of the material in the thickness direction. Nearly all residual elements adversely affect the crystallographic textures and the r-value of cold rolled and annealed steel. Tin and Arsenic also have adverse effects on recrystallization kinetics during the continuous annealing of cold rolled extra low carbon steel grades (Herman *et al*, 1996).

2.1.2 Beneficial effects of tramp elements

Self-alloying refers to the possibility of using the existing residuals as alloying elements. Several tramp elements exist in recycled steel in quantities enough to serve the alloying function. While in many cases the individual elements may not influence it enough, in combination, they may be effective in strengthening steel (Christian, 2007). Tramp elements may strengthen steel in several ways which in general reduce or inhibit mobility of dislocations:

a) Through transformation hardening, in which a microstructure of ferrite with varying levels of martensite is formed. The varying quantities of martensite allow for varying levels of strength. The strengthening process consists of heating steel so that the iron is converted to the face cubic centered (ganma) form, austenite, which dissolves up to 2% carbon. On suddenly cooling during quenching, the solubility of carbon is reduced and the formation of body centered cubic ferrite is not possible because of time limitations; instead, martensite, a super saturated body centered tetragonal form results. This features extreme hardness due to the martensitic distorted crystal structure which introduces crystal lattice defects that act as barriers to dislocation slip in proportions dependent on martensite volume fraction (Avramovic *et al*, 2008). This is the basis of the all-important steel property of hardenability.

The use of processes involving the rolling, quenching and tempering of steel bars in order to attain higher yield stress reinforcement bars bases vitally on hardenability, which is the indication of how deep into the material a predetermined hardness level can be achieved due to quenching. It is the feature behind transformation hardening and is chiefly dependent on the steel manganese and carbon contents although all tramp elements also affect the hardenability of steel though the reduction of the austenite transformation temperature as well as reducing the critical temperatures (Gregg *et al*, 2004).

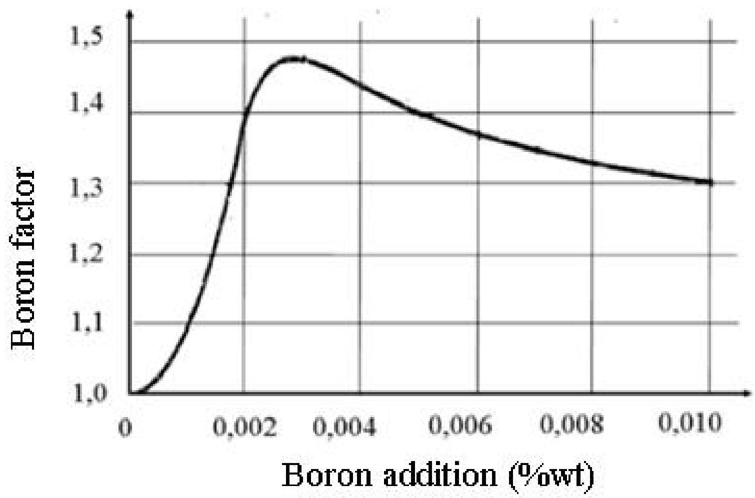

Fig 2. 6: Effect of Boron on Hardenability of Steel (Pirowski, 2007)

Substantial research has been done on the effect of these very small elemental containments in steel on hardenability.

According to Marcel Grossmann (1936), the effect of Boron may be expressed quantitatively as the Boron factor B_f, which is the ratio of the ideal diameters, Di, for the steel with and without boron as:

$$B_f = \frac{D_i \text{ with Boron}}{D_i \text{ without Boron}} \quad \ldots\ldots\ldots\ldots\ldots\ldots\ldots\ldots 2.4$$

Porowski *et al*, 2007 in their publication 'Micro Addition of Boron and Vanadium in Austempering of Ductile Iron' submit that 0.003% Boron in steel will have a hardenability factor of over 1.4 (Fig.2.7) although this effect was noted to be in inverse proportion to the steel carbon content (Fig.2.8) and also depended on the removal of Nitrogen with which Boron would otherwise preferentially form nitrides and complete deoxidation of the steel to avert Boron oxidation tendencies.

The solubility of Boron in iron-γ is almost zero but is influenced by the impurities present. Because of its low solubility in austenite, Boron can be highly concentrated in grain boundaries.

Mehran (2007) adds that when Boron bearing steel is cooled from the hardening temperature, the solubility of Boron is reduced. This results in even greater concentration of Boron at the grain boundaries. Minute grains of Boron carbide $Fe_{23}(BC)_6$ are subsequently formed there and to some extent they assume an orientation coherent with one of the two austenite grains between them which separate out. Atomic contact is thereby established between $Fe_{23}(BC)_6$ and austenite, resulting in a reduction in the surface tension and grain-boundary energy. The presence of Boron in solid solution and coherent Boron carbide in the grain boundaries delays the formation of ferrite and pearlite and also to some extent, bainite in preference to lower temperature forming martensite; hence increasing the hardenability of the steel.

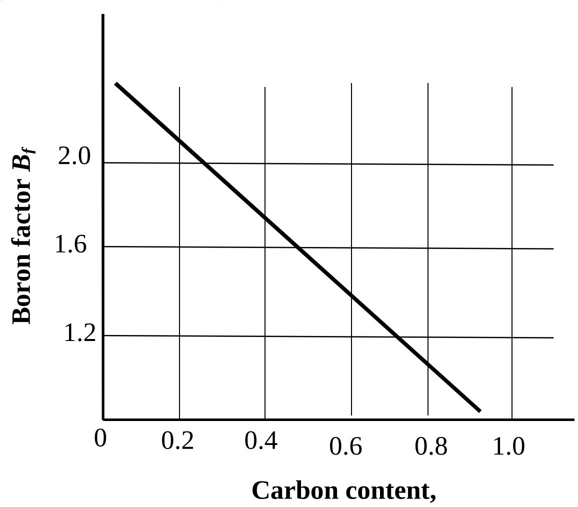

Fig 2. 7: Effect of carbon content on boron factor (Pirowski, 2007)

Boron enters the recycling process through Boron laden scrap. In steel scrap, Boron, usually in the range of 10 to 30 ppm, is sometimes utilized in steel to improve the hardenability of medium carbon steel with up to 0.3%C (Naro *et al*, 2004). Ferro-silicon and other additives also sometimes contain Boron as residual.

The principal source of Boron in the recycling practice in this country however, is the boric acid binding in the induction furnace crucible and ladle linings. The acid ramming mass is generally used in the induction furnace relining in the steel recycling industry. The silicon dioxide (SiO_2) is bound with boric acid (H_3BO_3) and is often factory pre-mixed. By adding small amounts of boric acid or boron oxide, the melting point of the silica is lowered, creating a borosilicate glass which cements the lining together. This, however, is a ready source of up to about 0.0028% (Brown, 2001). Boric oxide (B_2O_3) is reduced by silicon (and carbon at high temperature) and Boron is dissolved in the liquid iron (Jenkins, 2001).

Porowski also added that the presence of up to 0.04% Vanadium would analogously cause a hardenability factor of 1.4 (Fig.2.9).

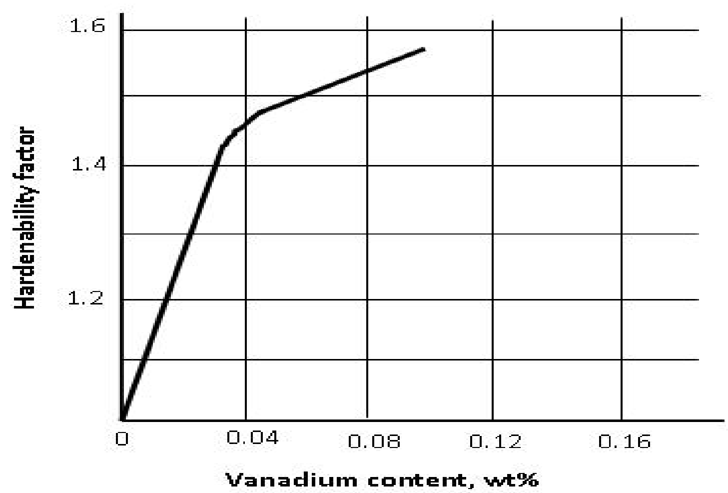

Fig 2. 8: Effect of vanadium on hardenability (Porowski, 2007)

Grange *et al* (1977) in their publication 'Hardness of Tempered Martensite in Carbon and Low Alloy Steels' had earlier submitted that alloying elements have individual hardening effects that are additive and increase with particular alloying element content. This was confirmed by Spies, 1992 in his paper 'Mechanical Properties of Ferrous and Nonferrous Alloys after Quenching, Theory and Technology of Quenching' with the equation:

$$HB = 2.84H_h + 75(\%C) - 0.75(\%Si) + 14.25(\%Mn) + 14.77(\%Cr) + 128.22(\%Mo) - 54(\%V) - 0.55(T_t) + 435.66 \ldots \ldots (2.5)$$

where *HB* is the hardness after hardening and tempering, H_h the hardness after quenching and T_t the hardening temperature.

The tramp element content naturally uplifts the steel carbon equivalent and the steel hardenability as a consequence as in equation 2.6 where Boron features predominantly in accordance to Yurioka *et al* (1985).

$$C_{eq} = C + A(C) * \{Si/24 + Mn/6 + Cu/15 + Ni/20 + (Cr + Nb + V + Mo)/5 + 5B\} \ldots \ldots (2.6),$$

where: $A(C) = 0.75 + 0.25tanh\{20(C - 0.12)\}$

Additionally, almost all alloying/tramp elements that enter into solid solution with austenite (with the exception of Cobalt and Aluminium) tend to reduce M_s and M_f temperatures (Fig.2.10),

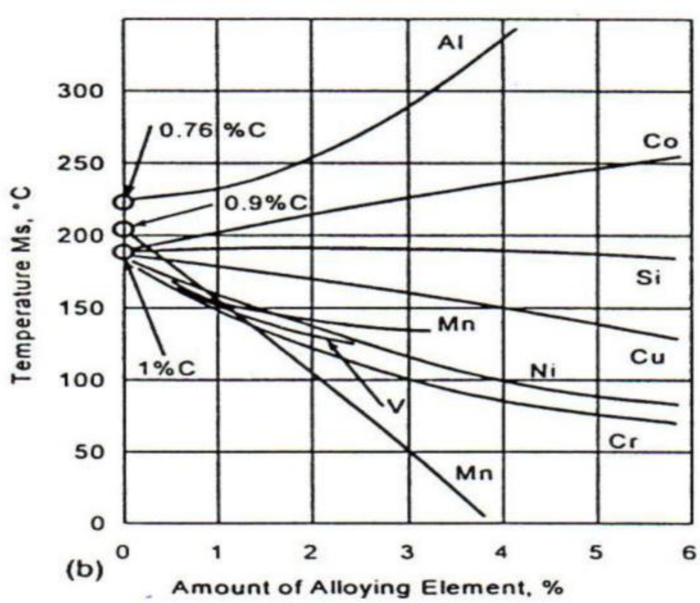

Fig 2. 9: Effect of alloying elements on martensite transformation

making it easier for martensite to form deeper in the section and at lower temperatures and increasing the dislocation density in the martensite. Tramp elements also reduce the critical cooling rate with a similar effect (Chong, 2008).

On top of this, alloying elements also retard the rate of softening during tempering by stabilizing both the transition carbides (e.g. $\mathcal{E}$-iron carbide) and the supersaturated martensitic structure to higher tempering temperature and by delaying considerably the precipitation and growth of cementite (Mehran, 2007).

b) In solid solution strengthening which occurs when the solute and solvent atoms defer in size and the solute atoms take positions in solvent lattices, causing distortion through the introduction of compressive or tensile stresses to the lattice depending on the solute atomic size relative to that of the solvent. These distortions impede dislocation motion and multiplication by interfering with nearby dislocations, making the solute atoms to act as pinning points; thus increasing the yield stress of the material (Buehler, 2005).

Depending on the atomic size of the alloying element, a substitutional solid solution or an interstitial solid solution can form. According to the Hume-Rothery size factor rule, if the solute differs in its atomic size by more than about 15% from the host, then it is likely to have a low solubility in that metal (Krishna,2007). Additionally, if the solute has a large difference in electro-negativity or electro-positivity compared to the solvent, then it is more likely to form an intermetallic compound. Its solubility would therefore be limited.

The shear-stress $\Delta\tau$ required to move dislocations in iron is proportional to the half-root of the solute (tramp) element concentration as in equation 2.7 (Meyers *et al*, 2009).

$$\Delta\tau = Gb\epsilon^{3/2}\sqrt{c} \ldots\ldots\ldots\ldots\ldots\ldots\ldots\ldots\ldots\ldots\ldots \quad (2.7)$$

where *c* is the tramp element concentration, ϵ is strain on the material caused by the solute, *G* is the shear modulus and *b* the Burgers vector. This equation points out the dependence of solid solution strengthening on the concentration of solute atoms, their shear modulus besides their valency.

c) In precipitation hardening, which results from the presence of solutes above a certain concentration so that second phase particles (precipitates) are formed that are a chemical combination between these solute atoms and other component element atoms present in the system such as iron in this case. The presence of second phase particles causes lattice distortions which appear when the precipitate particles differ in size and crystallographic structure from those of the host atoms (Caoa *et al*, 2006). The particles of the second phase precipitates act as pinning points just like solutes, impeding the movement of dislocations through the lattice and causing precipitation hardening (strengthening).

Two modes of precipitation strengthening can occur:

The dislocations can cut through the second phase particles in the process of their movement and the stress needed to cut though would be given as:

$$\tau = \frac{\pi r \gamma}{bL} \dots\dots\dots\dots\dots \dots (2.8)$$

where τ is the strength of the material the surface energy, *b* the Burgers vector and *L* the space between the pinning points where *r* is the radius of the second phase particle.
Alternatively the dislocations can bow around the particle (Orowan strengthening) requiring a stress:

$$\tau = \frac{Gb}{L-2r} \dots\dots\dots\dots\dots (2.9)$$

This bowing would result in the production of dislocation loops around the second phase particles leading to dense intertwining of dislocations and consequent hardening.
Equations 2.8 and 2.9 show that for small values of *r* corresponding to small grain second phase particles, the tendency for dislocations to cut though would dominate while for bigger particle size with larger values of *r*, the tendency to loop would dominate. Ultimately, the effectiveness of solid solution strengthening depends upon the size and modulus mismatch between foreign atoms and parent atoms (Mehran, 2007). The strengthening achieved by substitutional solute atoms is, in general, greater the larger the difference in atomic size of the solute from that of iron if one considers the Hume-Rothery size effect. Fleischer and Takeuchi however point out that the differences in the elastic behavior of solute and solvent atoms are also important in determining the overall strengthening achieved.

In their research titled 'Characteristic features of Titanium, Vanadium and Niobium as Micro Alloy Additions in Steel,' Nibinfo *et al* (1998) point out that the elements in groups 4 to 6 and periods IVA to VIA have a high potential to form nitrides and carbides. These carbo-nitrides tend to precipitate at the grain boundary and impose impediment to dislocation motion. These elements include Titanium, Vanadium, Chromium, Niobium and Molybdenum, Zirconium, Hafnium, and Tungsten which are also outstanding tramp elements in recycled steel. These precipitate particles which actually influence the microstructure of the steel are formed during hot working for which reason the tramp elements need to be in solid solution in austenite during preheating and rolling phases.

This solubility is strongly influenced by the difference in atomic size compared to the iron atom. Thus Zirconium and Hafnium with large atomic size differences of 25 and 31.3% from iron respectively, are not readily soluble in austenite and in spite of being strong nitride/carbide formers, do not affect steel microstructure (Nibinfo *et al*, 1998).

d) Through grain size effect, the strength of steel can also be controlled. Grain boundaries arise because of varying crystallographic orientations. During deformation, grain boundaries impede dislocation motion, making slip more difficult since the dislocations would need to change direction to suit crystallographic orientation and also negotiate though the discontinuity of slip planes associated with grain boundaries (Jubleanu, 2009). The number of dislocations per grain decreases with decline in grain size. The reduced number of dislocations per grain with smaller grain size results in fewer dislocations at grain boundaries, making it more difficult for dislocations to move into neighboring grains and leading to increased yield of the material as depicted in the Hall-Petch relationship:

$$\sigma_y = \sigma_{y,0} + \frac{k}{d^{1/2}} \ldots\ldots\ldots\ldots\ldots\ldots\ldots\ldots\ldots\ldots\ldots\ldots (2.10)$$

where k is is the strengthening coefficient, d is the average grain diameter and $\sigma_{y,0}$ the original yield stress representing the resistance to dislocation motion (Smith *et al*., 2006).

Vanadium for example, will be dissolved in austenite until γ-α transformation and will therefore not influence austenite grain size until then. Being precipitated at these low temperatures, the resulting grains are very fine and are able to strengthen steel when finally deposited on the austenite grain boundary. They also prevent further grain growth, leading to further strengthening (Nibinfo *et al* (1998). Thus Ferrite grain refinement in ferrite-pearlite steels is accomplished through restricting of the growth of austenite grains during hot rolling and/or by inhibiting the recrystallization of austenite during hot rolling so that the $\gamma \rightarrow \alpha$ transformation occurs in unrecrystalized austenite (Mehan, 2007).

In most instances, all V, T and Nb are in solution at the start of the hot rolling of austenite, but precipitation occurs during the rolling as the temperature of the steel drops. The precipitate particles hinder growth of austenite grains, and at still lower temperatures the particles (or precipitation clusters) inhibit recrystallization of the deformed austenite grains. The effectiveness of alloying (tramp) elements in refining ferrite grains is in the same order as the solubility of their carbides in austenite and as shown in Fig.2.11, the grain refining effect is in the order Vanadium, Titanium and Niobium (Mehan, 2007).

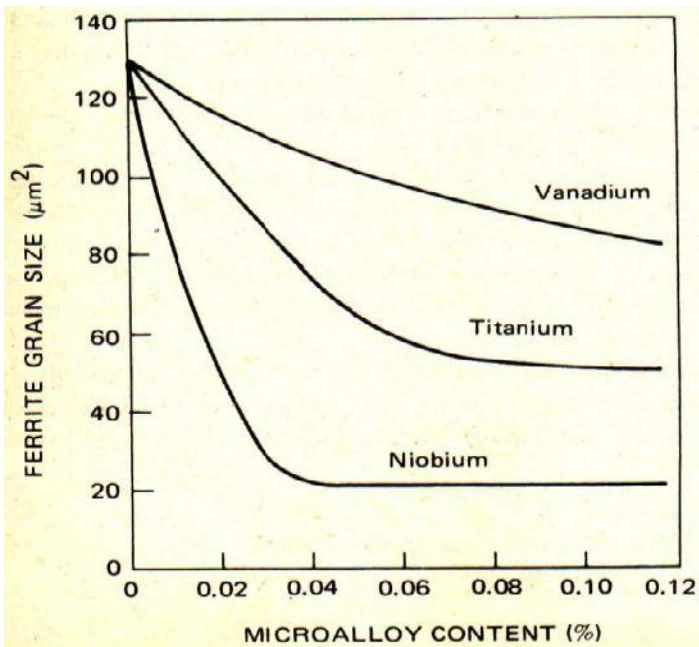

Fig 2. 10: Effect of tramp element content on grain size (Mehan, 2007).

e) Work hardening is an important strengthening process in steel, particularly in obtaining high strength levels in rod and wire both in plain carbon and alloy steels. The main feature responsible for work hardening is dislocations. Dislocations interact with each other by generating stress fields in the material (Wencora *et al,* 2005). The interaction between the stress fields of dislocations impedes dislocation motion by repulsive or attractive interactions. Additionally, if two dislocations cross, dislocation line entanglement occurs, causing the formation of jogs which oppose dislocation motion. These entanglements and jogs act as pinning points, which oppose dislocation motion. As both of these processes are more likely to occur when more dislocations are present, there is a correlation between dislocation density and yield strength as shown in the equation:

$$\Delta\sigma_y = Gb\sqrt{\rho_\perp} \ldots\ldots\ldots\ldots\ldots\ldots\ldots\ldots\ldots\ldots\ldots .2.11$$

where G is the shear modulus, b is the Burgers vector, and $\rho_\perp$ the dislocation density.

Increasing the dislocation density thus increases the yield strength which results in a higher shear stress required to move the dislocations.

In crystalline materials, dislocations are capable of traveling throughout the lattice when relatively small stresses are applied. This movement of dislocations results in the material plastically deforming. Pinning points in the material tend to halt dislocation movement, requiring greater stress to overcome the barrier. This results in an overall strengthening of materials. Dislocations would require proper lattice ordering to move through a material. Point defects, stationary dislocations, jogs and kinks in a material create stress fields within a material that prevent traveling dislocations from coming into direct contact. The dislocations are thus repelled from the already existing stress fields (Honeycombe, 2006).

The introduction of foreign atoms into a crystal naturally creates pinning points in the material because alloy (tramp) element atoms are inherently point defects and thus create stress fields when placed into a crystallographic position and so block the passage of dislocations. Even if the alloying atom were the same size as the host material and did not stress the lattice, it would have a different elastic modulus which would create different terrains for the moving dislocation and stop dislocation movement (Wang *et al*, 2013).

The precipitation of a second phase within the crystal of a material due to the presence of large amounts of tramp elements similarly creates physical blockades through which a dislocation cannot pass. As a result, the dislocations must bend, requiring greater stress to move around the precipitates.

2.3 Product Modes

2.3.1 Thermo-mechanically treated bars

Thermo-mechanical processing or ‘quenching and tempering’ is a metallurgical procedure that integrates rolling and heat-treatment into a single process in order to produce composite steel bar (Fig.2.12). The use of the thermo-mechanical treatment process has not only helped produce bars of high yield strength of 500Mpa and above but also with superior ductility, weldability, bendability, better corrosion and thermal resistance (Prabir, 2004). The reinforcement bar, after being successively rolled into the intended shape and size, is quenched at a controlled rate, producing a tough, high strength product from inexpensive low carbon steel. The quenching converts the billet surface layer to fine grained martensite (Fig.2.13) and causes it to shrink, pressurizing the core and helping to minimize grain size in neighboring crystal structures by deforming the grains in the intermediate layers (Monideepa *et al*, 2012) . The quenched layers are simultaneously tempered using the heat from the bar core. The core remains hot and austenitic. A microprocessor controls the water flow to the quench box to manage the temperature difference through the cross-section of the bars. The correct temperature difference ensures that all processes occur and bars have the necessary mechanical properties.

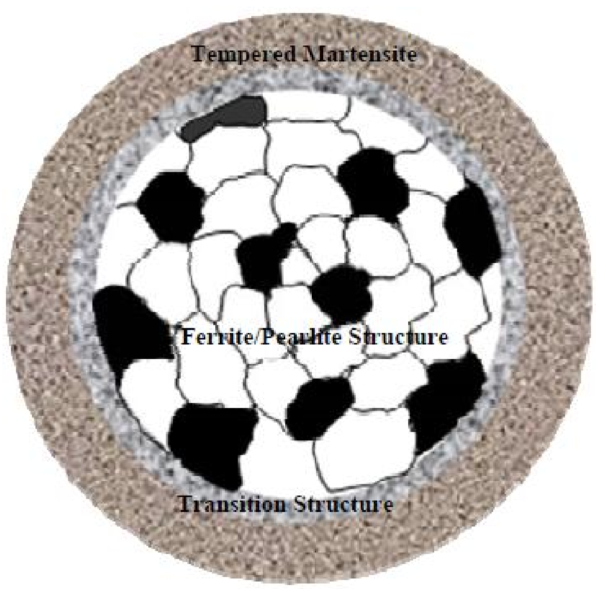

Fig 2. 11 Layers in the TMT Bar (Islam, 2012)

The bar leaves the quench box with a temperature gradient through its cross section. As it cools, heat flows from the bar centre to its surface so that heat correctly tempers an intermediate ring of martensite and bainite and ensures that the ultimate equalization temperature is set at 600°C (Fig. 2.15); ensuring that the resultant soft core constitutes about 65-75 per cent of the overall cross section area, depending upon the desired minimum yield strength, the rest being the hardened periphery (Tamm *et al*, 2010).

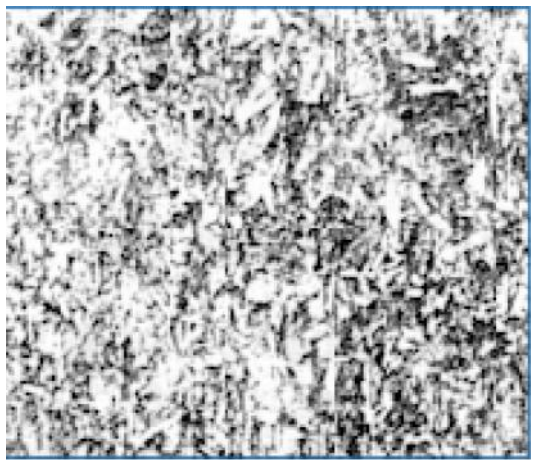

Fig 2.12: Fine Grained Tempered Martensite Rim (Islam, 2012)

Finally, the slow cooling after quenching automatically tempers the austenitic core to ferrite and pearlite (Fig.2.14) on the cooling bed. These bars therefore exhibit a variation in microstructure in their cross section, having strong, tough, tempered martensite outer ring to constitute the surface layer of the bar, an intermediate semi-tempered middle ring of martensite and bainite, and a refined, tough and ductile ferrite and pearlite circular core (Fig.2.12). This is the desired micro structure (Markan, 2004). The relatively small grain size is essential for the strong and tough exterior of the TMT reinforcement bar since the strength of steel is proportional to the grain size (Fig.2.16).

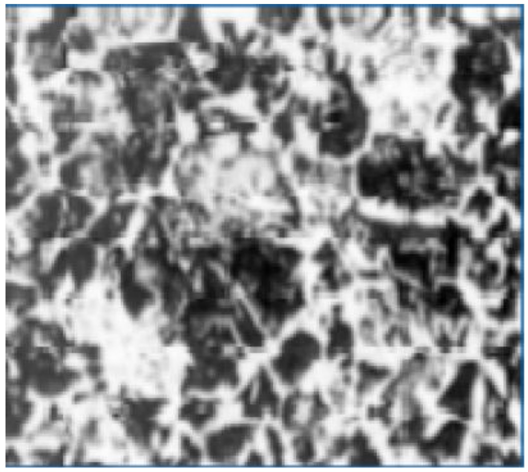

Fig 2. 13: Ferrite-Pearlite Core in TMT bar(Islam, 2012)

2.3.2 Twisted reinforcement bars

Following the rolling process referred to earlier (Fig.2.2), the bars destined for cold twisting are allowed to cool to room temperature, held in chucks at each end and subjected to a twisting moment until a helix angle of about 25 degrees is obtained in order to achieve the 415Mpa yield requirement as well as the essential concrete anchorage. This being a cold working process, it is accompanied by a substantial residual stress build up (Tian *et al*, 2010). The major short comings of twisted bars are essentially related to this factor since corrosion resistance, limited ductility, limited weldability are all due to residual stresses in one way or another. The fact that work hardening is the result of cold working brings with it the result that twisted bars lose their strength upon being heated above recrystallization temperature. This heating process takes place during the usual heating and bending often done on building sites in order to achieve mechanical anchorage.

All the different applications of steel bars described are influenced by the quality of steel which ultimately determines the effectiveness with which they are able to carry out their designated functions. The quality of steel is the completeness with which it satisfies the expected properties with which it manifests its usefulness for purposes of specific predetermined engineering values (Tupkary, 2008).

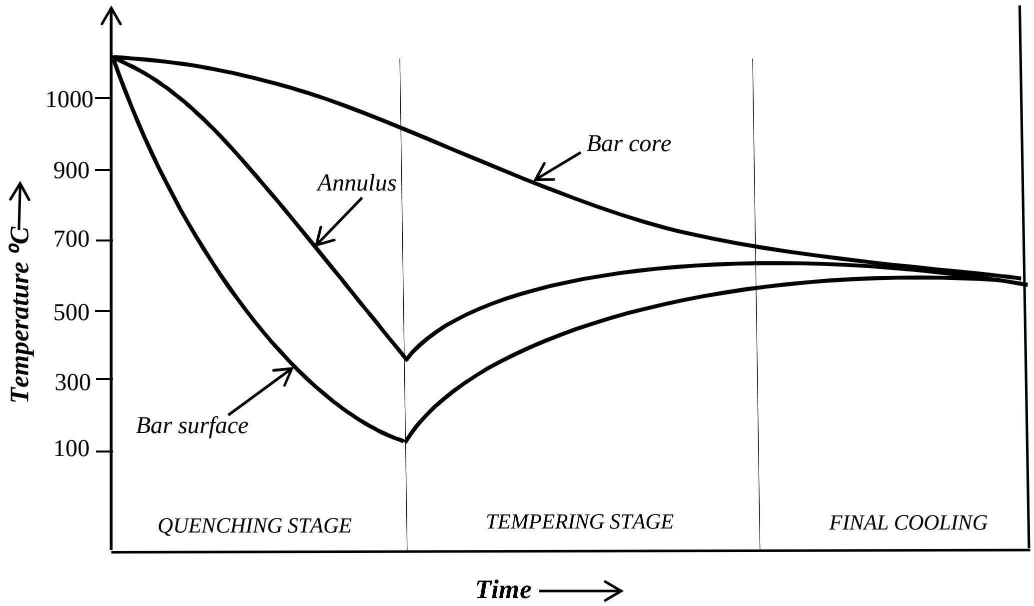

Fig 2. 14: Temp.-Time Diag. for TMT Cooling Process (Markan, 2004)

The purpose of the present work is to examine the extent to which the use of recycled steel affects the properties of steel and raise possible solutions to address the consequent shortcomings. Among others, these properties are strength, hardness, ductility, hardenability and weldability. These have been addressed in five papers.

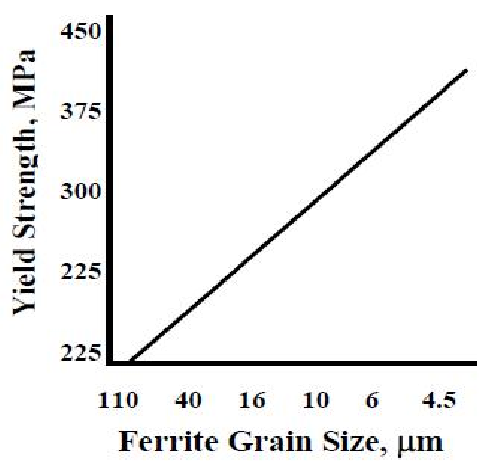

Fig 2. 15: Ferrite Size vs Steel Bar Yield (Islam, 2012)

2.4 Reinforcement of Concrete with Steel

In reinforced concrete construction, the efficiency with which forces are transmitted between the steel reinforcement and concrete is the most important feature in the effectiveness of the resulting composite and is determined by the bond between reinforcing bars and concrete (Fang *et al*, 2004). This in turn depends on the chemical adhesion between the bar and the concrete, frictional forces arising from the roughness of the steel-concrete interface and mechanical anchorage offered by the bar ribs against the concrete surface (Ismaeel *et al*, 2013).

Chemical adhesion mainly plays its part at relatively low stress levels. Once adhesion is lost at higher stresses, if any movement between the reinforcement and the concrete occurs, bond is then provided by friction and the anchorage on the ribs of the bar. At much higher bar stress, however, bond strength is fostered entirely by concrete anchorage on the bar ribs (Mongkol, 2008)**.**

Considering a typical beam under flexural loading (Fig.2.17), the bending moment on the beam creates tensional stresses which in turn result in bond stresses between concrete and the reinforcement. These stresses are finally translated into compressive stresses *c* acting perpendicular to the bar rib flanks and bearing forces *f* along the bar rib flanks inclined to the longitudinal axis of the bar at an angle α (Fig. 2.18).

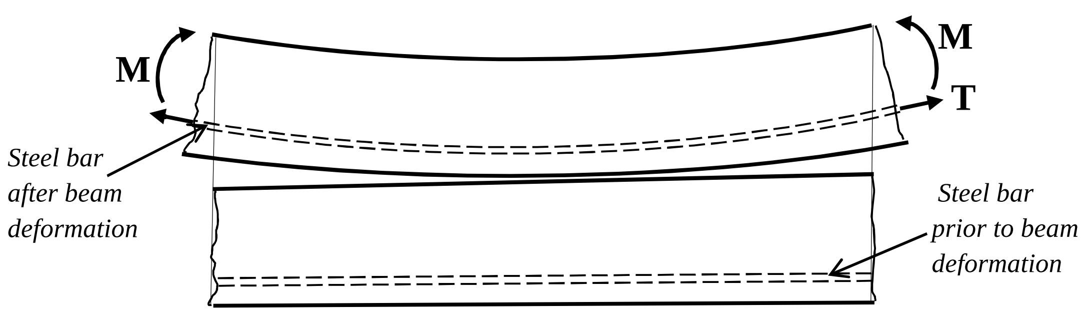

Fig 2.16: Action of moments and forces on reinforcement on bending

These resolve into radial (hoop stresses) and longitudinal components ρ and λ respectively (Fig.2.18). The radial stresses ρ cause circumferential stresses around the bar, which may generate splitting failure (Fig.2.19). The load at which splitting failure develops is a function of the minimum distance from the bar to the surface of the concrete or to the next bar, the tensile strength of the concrete and the average bond stress (Nawy, 2004). In general, the smaller the distance from the concrete surface, the smaller is the required splitting load.

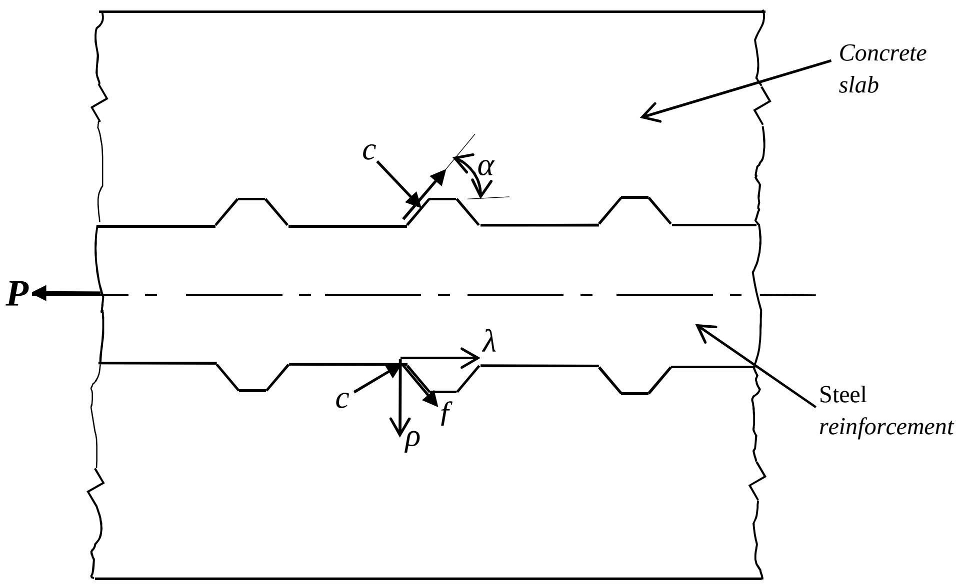

Fig 2.17: Bearing forces on bar ribs

If these conditions are not met, splitting does not occur and instead, pullout failure due to the longitudinal stress *λ* ensues. In that case the bar and the ring of concrete between successive bar ribs pullout along a cylindrical failure surface joining the tips of the ribs so that the concrete shears parallel to the bar axis; the resultant crack propagating to the surface of the concrete element (Fig 2.20).

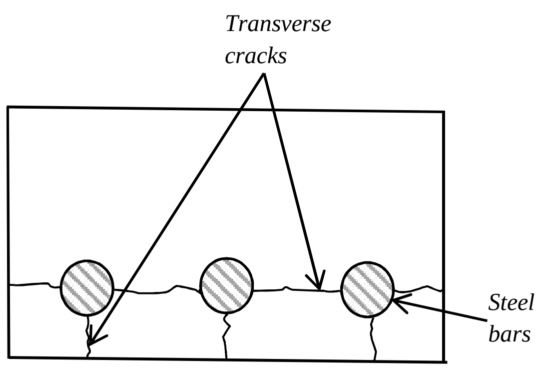

Fig 2.18: Splitting failure in reinforced

As slip progresses, the stress in the reinforcement reduces to zero and the beam subsequently behaves like plain concrete, giving in to immediate failure in a typical fragile mode. Since the purpose of reinforcing concrete is to impart ductility values otherwise unavailable in concrete alone, it is at this stage that the pullout can be prevented by designing the steel bar as the weaker element in the concrete-steel chain for if anchorage to the concrete is sufficient, the stress in the reinforcement should become high enough to lead the steel bar to its yield value.

Bond stresses oppose the propensity of the steel bar to being pulled out of the concrete. They exist whenever the force in the reinforcing bar changes from one location to another along the bar.

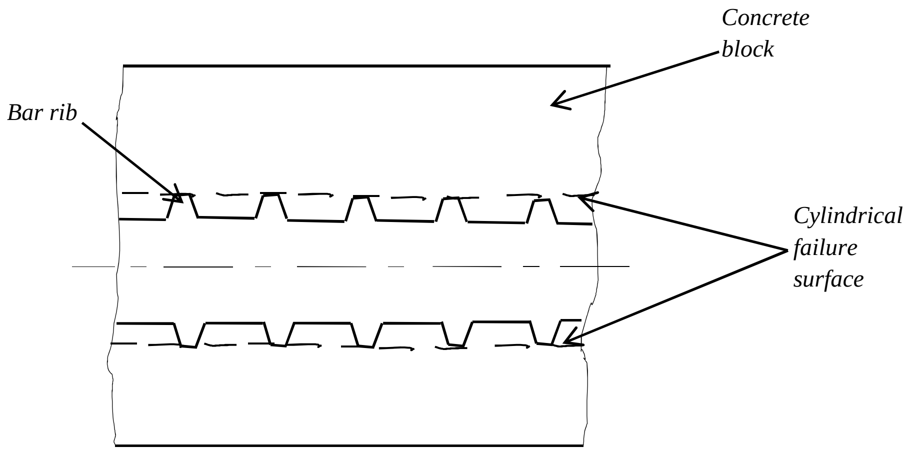

Fig 2.19: Pull out failure in reinforced

The development length, l_d is the length of the reinforcement bar anchorage that will cause bond stresses equal to the yield stress of the reinforcement bar (ACI 318-08). For ductile failure of the concrete steel composite (Fig.2.21), it necessary to make the steel bar the weaker part of the linkage. This is achieved when the shear stress in the concrete needed for pull out should be greater than the steel bar yield stress, that is; $\sigma \leq \tau$;

$\tau = P/\pi d_b l_d \leq \tau_c$ …………………………………………..2.12)

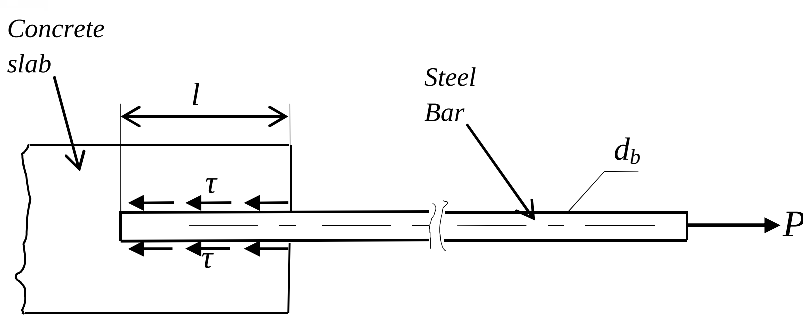

Fig 2.20: Development length and the action of shear stresses

$$\sigma = \frac{4P}{\pi d_b^2} \leq \sigma_y \ldots\ldots\ldots\ldots\ldots\ldots\ldots\ldots\ldots\ldots.2.13)$$

Combining *2.12* and *2.13*,

$$\pi d_b l_d \tau_c \geq \sigma_y \pi d_b^2/4$$

and

$$l_d \geq \left(\frac{\sigma_y}{\tau_c}\right)\frac{d_b}{4} \ldots\ldots\ldots\ldots\ldots\ldots\ldots\ldots\ldots\ldots\ldots\ldots\ldots\ldots\ldots 2.14)$$

where:

l_d is the development length.

σ_Y the yield stress of the steel reinforce bar.

τ_c the allowable (limiting) concrete shear stress at the concrete/steel interface.

d_b the diameter of the steel bar at rib height.

Equation *iii)* shows that the value of σ_Y/τ_c determines l_d for a given bar diameter and that the value of l_d increases lineally with σ_Y.

This is also in conformity with the American Concrete Institute (ACI) development length in equation *iv)* ACI 318-08, equation 12-1.

$$l_d = \frac{1}{3.5}\left[\frac{f_y}{\lambda\sqrt{f_c'}}\right]\left[\frac{\Psi_t\Psi_e\Psi_s}{\left(\frac{C_b + K_{tr}}{d_b}\right)}\right] d_b \ldots\ldots\ldots\ldots\ldots\ldots\ldots\ldots\ldots\ldots\ldots.2.15)$$

in which

f_y is the yield stress of the steel bar(σ_y).

f'_c the specified comprehensive strength of the concrete.

Ψ_t is takes into account the location of the bar relative to the concrete surface.

Ψ_e is a factor considering the coating on the bar (surface finish).

Ψ_e takes the size of the bar into account.

λ is the aggregate factor.

There are several concrete types in use in the civil engineering practice and most common of all are normal concrete, high strength concrete, high performance concrete (ARC,2008). To each of these types, there is a corresponding value of the allowable stress, τ_c. For the purpose of this study, concrete refers to normal concrete variety (normal weight or normal strength concrete) with a yield point of up to 40MPa.

The high strength Thermo-Mechanically Treated (TMT) bars are of minimum of 460 MPa upper yield (US 155-2). Higher yields are limited to 550 MPa for longitudinal reinforcement (ACI 318-08, 2008) and projections are normally based on this strength maximum level. To make the bar the weaker part of the steel-concrete composite link, the yield strength of the bar must be within certain limits for a given type of concrete so as to facilitate a pre-calculation of the development length. In this research, the extent to which recycled steel is able to conform to this requirement was examined.

CHAPTER THREE: METHODOLOGY

3.1 State of the Industry

The state of the Ugandan steel industry was investigated in Paper 1. Data was collected through industrial visits and individual interviews at different steel mills, foundries and related metal products user industries and stakeholders. Extensive review of relevant literature was also done.

3.2 Sample Selection

Thirty steel bars were collected one per day, from six different mills located in different parts of the country as shown in the map in Fig. 3.2 to represent a month's production in each case. Out of the resulting 180 bars, a total of 80 samples were thermo-mechanically treated (TMT) bars examined in Paper 5 while 30 others were twisted bars studied in Paper 3. The rest of the bars were plain square bars for experimentation in Paper 2 and Paper 4. This is schematically shown in Fig. 3.3 and 3.4.

3.3 General Properties of Steel

For Paper 2, hot rolled plain square bars were subjected to tensile testing by cutting 300mm lengths from them and loading the pieces monotonically using MFL SYSTEM hydraulic universal tensile testing machine. The corresponding load-extension diagrams were machine plotted. Their yield and ultimate stresses and percentage elongation values were computed using actual cross sections. Test lengths of five times the length of the side of the square section were used as dictated by US 155-2.

Lengths of 5mm were cut and ground flat for spectrometry done with *SPECTROL AB* spark spectrometer.

Lengths of 10mm were cut and micro-polished with aluminium oxide powder. Micrographs were also photographed with an *OLYMPUS-412* light microscope.

The torque at yield and at fracture and the maximum angles of twist of 300mm lengths of the bars were also determined using an *AVERY* 6609 torsion testing machine and a bevel protractor. All tests were done in accordance with the EAS 412-1:2005 (ISO 6892).

3.4 Reinforcement with Twisted Bars

For paper 3, bar lengths of 300mm were cut from 6m length of 18 reinforcement twisted bars of 20mm, 16mm, 12mm and 10mm square section selected from diverse steel outlets in the country. Their ultimate and yield strengths were tested on unmachined samples using *MFL SYSTEM* hydraulic universal tensile testing machine in accordance to the EAS 412-1:2005 (ISO 6892). The samples for tensile testing were cut one from each end and one from the middle of the 6m steel bars. The yield strength σ_u and ultimate strength σ_y were computed with the initial cross-section area.

The cross section area A was calculated by determining the weight (*w*) of a known length (*l*) of the bars of density ρ using the relationship $A = {}^{w}/_{\rho l}$.

The composition of samples from each of the bars was determined through spark emission spectrometry using *SPECTROL AB* apparatus and five bars with the highest yield stresses were analyzed.

Additionally, the yield strength of seventy-two recycled steel TMT reinforcement bars of diameters: 10, 12, 16, 20, 25 and 32mm from one manufacturer were determined. To do this, one bar was selected from each of the three shifts every day for 24 working days. The bars were monotonically loaded to failure in tension. Their yield stresses were determined using a *TESTOMATIC* tensile testing machine in accordance to US 155-2. Their chemical composition was also determined using *SPECTRO-APPARATUS* spark spectrometer.

The mean yield μ and the standard deviation σ were determined from the data and the frequency distribution curve plotted with the Microsoft Office Excel *XY*-chart accordingly. The cumulative distribution function $P(X \leq \chi)$ where χ was the 550Mpa limit was then calculated through the determination of the standard score $z = (\chi - \mu)/\sigma$ and use of the standard normal distribution tables. Thus $P(X \geq \chi) = 1 - P(X \leq \chi)$ where χ is the random variable (yield strength) was determined.

The yield strengths for samples above 550Mpa were also plotted against the Carbon, Manganese and Boron content and the line of best fit inserted in a Microsoft Excel format.

3.5 Weldability of Steel Bars

To study the weldability of the steel in Paper 4, two 150mm lengths were cut from each of the thirty pieces of the 10mm steel square bars. The cut off pieces were prepared for V-groove flat position welding and designed to have more width than depth as shown in Fig.3.1.

Single pass butt welds were made with 4mm diameter manual metal arc welding (MMA) rods (E6013) at 4mm per second using 198 Amps, 100 volts setting in accordance with US IEC 60974-1: 1998 443. The samples were left to cool in still air and examined for cracks after 24 hours.

The weld beads were subsequently ground down with a surface grinder and micro-finished with aluminium oxide powder. The surfaces were cleaned with petroleum distillate (mineral turpentine), treated with a red dye penetrant and later with calcium carbonate suspension in propanol/acetone as developer every after 48 hours for seven days. Transverse micro-hardness readings were taken with a Super Rockwell Duplex 713-SR hardness tester using a 1/16" ball with 100kgf in the HRb scale across the face of the selected samples at 1.5 mm intervals and hardness was plotted against transverse displacement.

The chemical composition of the four samples PV5, PV8, PV19 and PV26 which showed detectable cracks was also determined with a *SPECTROL AB* spark spectrometer.

Their Chromium equivalents were calculated as:

$$Cr_{eq} = Cr + 2Si + 1.5Mo + 5V + 5.5Al + 1.75Nb + 1.5Ti + 0.75W \dots\dots\dots\dots.. (3.1)$$

while the Nickel equivalents were determined as:

$$Ni_{Eq} = Ni + Co + 0.5Mn + 0.3Cu + 30C \dots\dots\dots (3.2)$$ (Antonio, 2009).

The corresponding carbon equivalents have been calculated as:

$$C_{eq} = C + A(C) * \{Si/24 + Mn/6 + Cu/15 + Ni/20 + (Cr + Nb + V + Mo)/5 + 5B\} \dots (\mathbf{3}.3)$$,

where:

$A(C) = 0.75 + 0.25tanh\{20(C - 0.12)\}$ (Yurioka *et al*., 1985).

Fig 3.1: Map of Uganda Showing Locations of Steel Mills

3.6 Thermo-Mechanically Treated Bars

Hardenabiltiy, a steel property and factor in the quality of steel was examined in Paper 5 with the help of thermo-mechanically treated bars. To do this, thirty pieces of 32mm nominal diameter (TMT) reinforcement bars selected from different steel plants in the country were tested. Micro-hardness measurements of cross-sections were carried out from surface to core on all the pieces using an *HR-500 MITUTOYO* Rockwell hardness tester. Tensile tests were carried out on the thirty pieces using *BLUE STAR UTN-(E) 100* Universal Testing Machine to EAS 412-1:2005 (ISO 6892) standard. Four of the samples were selected on the strength of their representative results. Additional hardness readings were taken of the samples to determine the hardness pattern on both extremes of the bar samples. The chemical composition was determined using a *SPECTROL LAB* spark spectrometer and the carbon equivalents calculated according to equation 3.3.

Bend tests were also conducted in accordance with East African standard, EAS 412-2-2008, using Φ200mm mandrel.

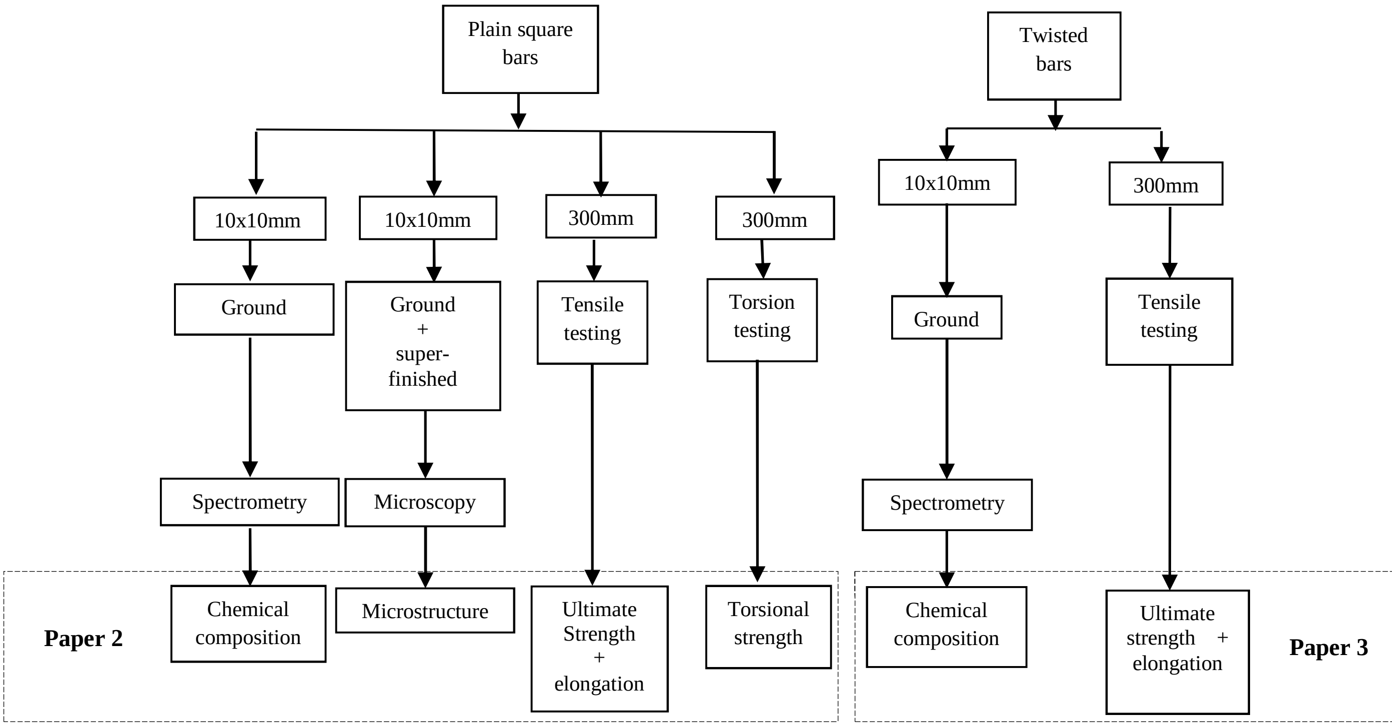

Fig 3. 2: Investigation Flow Chart for Steel Bars in Paper 2 and Paper 3

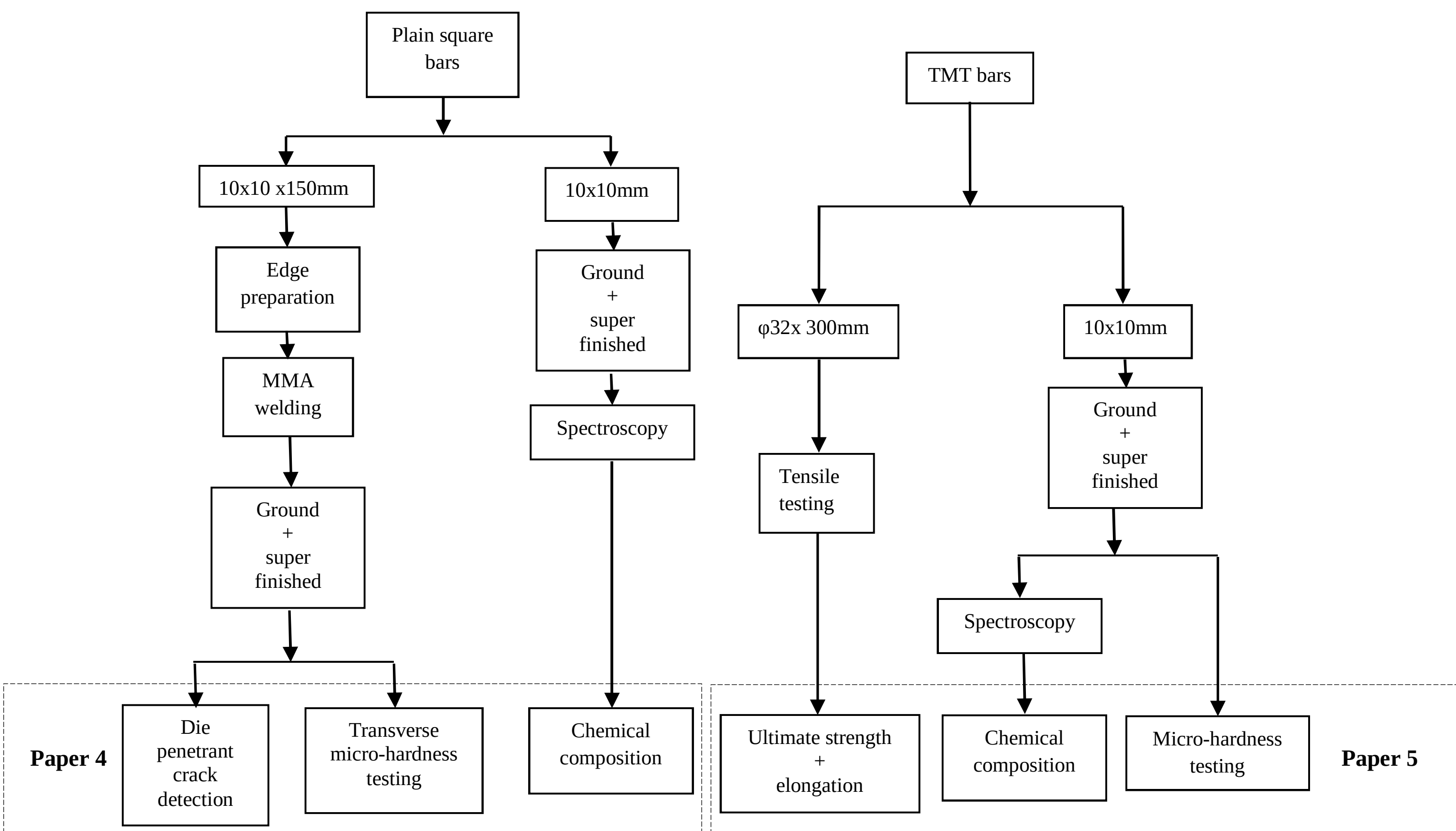

Fig 3. 3: Investigation Flow Chart for Steel Bars in Paper 4 and Paper 5

CHAPTER FOUR: RESULTS AND DISCUSSION

This chapter analyses the results of the study carried out on the general position of the industry and its production status as well as the analysis of the samples in their various groups in consonance with the Papers written on the strength of the major steel properties.

4.1 State of the Industry

The Ugandan steel industry as investigated in Paper 1 is characterized by mini mills with the electric furnace production. The induction furnace dominates the national production scene. The electric arc furnace (EAF) installed in two of the steel recycling mills are either underutilized or completely dormant. The Induction furnaces (IF) in both cases are substantially more active and at full capacity utilization in five out of the seven mills visited operating at three shifts a day. Mills were visited at Steel Rolling Mills (Ltd) in Jinja, Tembo Steel Rolling Mills at Lugazi and Iganga, Modern Steel International Ltd and Pramukh Steel Ltd both in Njeru, Jinja, Roofings Rolling Mills in Mukono District in addition to BMT Steel Rolling Mills at Mbarara. The production process is invariably affected by the low availability of scrap, the essential raw material whose low volume and poor quality present the largest problem to the melting industry. Until the recent ban on scrap exportation, the Kenyan steel recycling industry imported most of their scrap from Uganda, this has increased the cost of steel bars by 25%. The outstanding openings to the improvement of the quality of the input are geared towards the exploitation of the high quality iron deposits in the western part of the country which in turn depend on the future industrial level exploitation of the natural gas reductant in the Albertine zone.

The average total annual steel production shared between the seven active steel recycling plants over the last three years, standing at between 150,000 and 1700,000 metric tons per year is predisposed towards the elaboration of structural fabrication and steel reinforcement bars, making plain square bars for the former and twisted and ribbed (TMT) bars for the latter purpose. Only BMT was found using the steel for wire drawing. This figure is still far below the imported steel average standing at 260,000 metric tons (UBOS, 2006).

4.2 General Properties of Steel

4.2.1 Composition

The chemical examination of the plain square bars analyzed in Paper 2 was as illustrated in the Table 4.1(a) and 4.1(b) showing that carbon contents were all quite high for samples in group P reaching 0.51% in sample P11. Sample P20 however showed lower than standard carbon content. The carbon percentage in the group T was generally acceptable, tending to be low. Sample T30, however, recorded 0.51%C, a higher than standard carbon content while T5, T11, T14 and T23 were rather low. The sulphur and phosphorous levels were all correctly below the maximum standard percentage of 0.07%. The manganese content was also normal although P2 and T30 top their respective groups. The copper content was well above the 0.1% to 0.2% range for both series varying widely between 0.34% and 0.44%.

Table 4.1(a): Chemical Composition of Bars, Gp P

Sample	%C	%P	%S	%Cu	%Cr	%Mn
P2	0.31	0.002	0.020	0.37	0.34	0.74
P5	0.49	0.004	0.016	0.36	0.54	0.48
P8	0.37	0.005	0.017	0.42	0.25	0.53
P11	0.51	0.001	0.015	0.37	0.49	0.49
P14	0.28	0.001	0.013	0.36	0.27	0.49
P17	0.27	0.001	0.014	0.36	0.28	0.45
P20	0.23	0.003	0.014	0.44	0.21	0.55
P27	0.36	0.006	0.016	0.39	0.22	0.46
P28	0.37	0.008	0.017	0.45	0.17	0.50
P29	0.32	0.004	0.017	0.34	0.24	0.48

Table 4.1(b) Chemical Composition of Bars, Gp. T

Sample	%C	%P	%S	%Cu	%Cr	%Mn
T1	0.28	0.008	0.018	0.39	0.19	0.45
T5	0.24	0.006	0.016	0.41	0.14	0.53
T8	0.26	0.003	0.014	0.42	0.17	0.53
T11	0.24	0.006	0.017	0.36	0.15	0.49
T14	0.24	0.006	0.021	0.42	0.20	0.53
T19	0.30	0.012	0.019	0.38	0.16	0.44
T21	0.44	0.012	0.019	0.41	0.21	0.67
T23	0.21	0.007	0.017	0.34	0.14	0.59
T26	0.35	0.001	0.022	0.39	0.22	0.49
T30	0.51	0.07	0.025	0.39	0.13	0.61

Steel containing between 0.2%C and 0.6%C is expected to be between 320MPa and 500Mpa (Newby *et al*, 1989). This is largely fulfilled in Group T but superseded by most samples in group P as shown in Table 4.2(a) and 4.2(b) and is mainly due to the elevated carbon content and the presence of manganese and other carbide forming and ferrite strengthening elements. The EAS 412 (ISO 6935) however stipulates an average carbon content of 0.25≤%C≤0.27 which is violated by all samples analyzed in the P series except P17 and only fulfilled by one out of the ten samples in the T series.

Table 4.2(a): Mechanical, Geometrical Props, Gp. P

Sample	σ_u	σ_y	δ%	Δ*X/X%*	σ_u/σ_y
P2	549	333	19	-22	1.62
P5	629	382	14	-22	1.65
P8	576	347	24	-24	1.59
P11	647	389	20	-23	1.65
P14	552	343	19	-20	1.61
P17	543	339	22	-21	1.60
P20	554	311	26	-22	1.78
P27	512	295	24	-21	1.74
P28	507	325	28	-20	1.56
P29	531	316	16	-18	1.68

Due to varying amounts of sulfur in scrap of different origins, the ferromanganese quantities added to regulate it in the melt vary widely, resulting in similarly large variations in the manganese content in the steel, being 0.45≤%Mn≤0.74 for the P series and 0.44≤%Mn≤0.67 even though in both cases it remains within the required range.

The corresponding carbon equivalent values calculated as:

$$C_{eq} = C + Mn/6 + (Cr + V + Mo)/5 + (Cu + Ni)/15 \quad \ldots\ldots\ldots\ldots\ldots (4.1)$$

which has to conform to the $0.55 \leq C_{eq} \leq 0.57$ range according to EAS 412-1:2005, was in agreement for series T but only for P5, P8, and P11 in series P; leaving 70% of the samples out.

Table 4.2(b): Mechanical, Geometrical Props, Gp. T

Sample	σ_u	σ_y	δ%	Δ*X/X%*	σ_u/σ_y
T1	495	339	42	-24	1.46
T5	498	344	40	-21	1.44
T8	541	364	34	-18	1.49
T11	488	332	26	-27	1.47
T14	515	364	27	-24	1.41
T19	514	374	25	-21	1.37
T21	562	387	17	-21	1.46
T23	516	362	24	-23	1.43
T26	523	377	28	-19	1.37
T30	487	340	20	-21	1.43

Table 4.3: Torsion testing results

Sample	τ_{max}	σ_u / τ_{max}	Sample	τ_{max}	σ_u / τ_{max}
T1	354	1.40	P2	426	1.29
T5	420	1.19	P5	503	1.25
T8	431	1.26	P8	435	1.33
T11	393	1.24	P11	447	1.45
T14	418	1.23	P14	434	1.27
T19	359	1.44	P17	405	1.17
T21	428	1.32	P20	440	1.26
T23	377	1.37	P27	398	1.29
T26	377	1.39	P28	416	1.22
T30	245	1.99	P29	443	1.20

The high carbon content and carbon equivalent of the samples, while contributing to the elevated strength values, naturally makes them less ductile. In the case of P5 and P29 in Table 4.1(a) of carbon contents 0.49 and 0.32 respectively, the elongation values are actually less than the required 16%; leading to reduced bending (ductility) characteristics. Ductility is essential when steel bars are twisted into reinforcement bars and quite important in most fabrication applications.

Ductility is an expression of the capacity of a material to accept permanent deformation without fracture and is due to the process of shear (Kakani *et al*, 2006). During the shear process, particles change their neighbors under the action of external forces. Shear involves the rupture and reformation of inter-atomic bonds; a feature also known as dislocation motion. A major impediment to dislocation motion is the occurrence of interstitial elements like carbon and also substitutional atoms along with second phases often formed preferentially between carbon, nitrogen and many of the tramp elements (Satish, 2009). The resistive action to motion of these elements not only increases the critical resolved shear stress of the base material, but also creates a situation where maintaining the minimum of five independent slip systems is difficult. According to the von criterion, these slip systems must be operative for a polycrystalline solid to exhibit ductility and maintain grain boundary integrity necessary to for polycrystalline material to avoid rupture.

This is even clearer if one considers the many sources of dislocation pinning due to the large multitude of tramp elements in recycled steel (Raghavan , 2004).

In some cases there was a substantial difference in the chemical composition determined in pieces cut from the same sample (Table 4.4).

Table 4.1: Comparison of Strength at Bar Ends

Sample	P29/1	P29/3	P28/1	P28/3	T21/1	T21/3
σ_u	531	582	507	497	562	516
CE	0.449	0.618	0.540	0.521	0.642	0.564

This is due to the presence of multitudes of solutes (tramp elements) and deficient stirring especially in the teeming ladle, giving rise to a gradient in composition at different positions of the billet as it leaves the mold in the continuous caster (Tupkary *et al*, 2008).

Table 4.5 shows the chemical composition and some mechanical properties of 10mm square steel bars from two steel recycling mills in Nairobi, Kenya. A noticeable variability in the carbon and manganese and boron content as well as the yield values and the steel percentage elongation depicts the similarity in manufacturing difficulties in the steel made in these mini-mills and that made in Uganda.

Table 4.5: Composition and properties of steel from two mills in Nairobi

Sample	%C	%P	%S	%Cu	%Sn	%Ni	%Cr	%B	%Mn	σ_y	δ%
K1	0.28	0.041	0.052	0.304	0.041	0.106	0.126	0.0016	0.471	339	36
K2	0.35	0.062	0.072	0.384	0.053	0.139	0.122	0.0018	1.020	488	40
K3	0.23	0.042	0.063	0.306	0.033	0.090	0.078	0.0009	0.643	348	43
K4	0.52	0.052	0.052	0.284	0.027	0.102	0.271	0.0032	0.505	373	17
K5	0.37	0.043	0.048	0.305	0.031	0.083	0.128	0.0027	0.481	333	19

In Fig.4.6, the composition and mechanical properties of similar steel bars from South African manufactures is shown. The uniformity in the carbon content, phosphorus manganese, copper as well as yield and elongation values suggests definite superior manufacturing and quality control processes.

Table 4.6: Composition and properties of steel samples from South Africa

Sample	%C	%P	%S	%Cu	%Sn	%Ni	%Cr	%B	%Mn	σ_y	δ%
S1	0.24	0.047	0.05	0.247	0.035	0.09	0.140	0.0003	0.69	511	19
S2	0.24	0.043	0.04	0.243	0.029	0.82	0.094	0.0014	0.71	532	19
S3	0.21	0.046	0.05	0.284	0.034	0.11	0.108	0.0015	0.65	518	21
S4	0.23	0.040	0.04	0.266	0.031	0.09	0.100	0.0014	0.73	535	20
S5	0.23	0.038	0.04	0.246	0.029	0.09	0.087	0.0014	0.69	542	18

4.2.2 Microstructure

All the samples examined showed a fairy regular carbon steel microstructure with ferrite forming the matrix in which pearlite patches were distributed, giving generally ductile hot-worked structures although in some cases sharp grain boundary profiles were noticeable as in the case of P29 (Fig.4.5) explaining its relatively lower ductility in the group (δ=19) in table 4.2(a). Some of the samples had indications of directional grain tendencies (Fig.4.6). This is due to the irregular steel composition resulting from recycling scrap. All bars of a given size are given the same time during reheating yet bars with higher carbon and other carbide forming element content would need more time in the soaking zone during reheating to dissolve these elements in austenite prior to hot rolling otherwise a certain amount of micro-particle inhomogeneity is retained, causing detectable post rolling grain uniaxiality in properties and microstructure, reminiscent of cold rolling process (Yu Jin Jang *et al*, 2007).

In Fig.4.7, banding, which is a common tendency in hot rolled steels with high micro alloy (tramp) element content is evident.

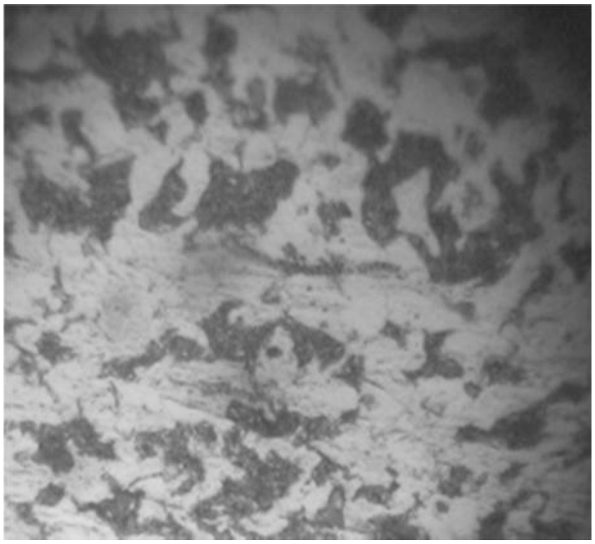

Fig 4.1: Sharp grain contour in P29

The formation of inter-dendritic chemical variations on solidification which never fully get homogenized on rolling but are rather modified in physical presentation with successive hot rolling enables them to be elongated in the direction of rolling, producing regions of high and low chemical solute concentration (Thompson *et al*., 1992). The alternating white and black bands in Fig.4.7 indicate the ferrite and cementite deposits. These are derived from the primary solvent (ferrite) dendrite formation and the posterior darker solute (cementite) in the liquid around the solidifying dendrites redistributed during subsequent rolling.

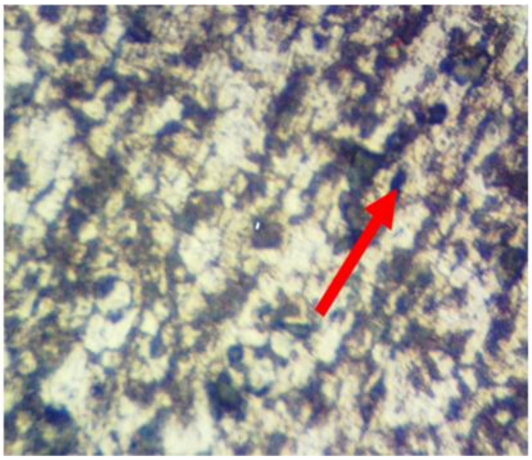

Fig 4.2: Directional grain tendency in P 5

Additionally, substitutional elements like manganese with characteristic low diffusion coefficients in iron respond slowly to the homogenizing, self-annealing effect of the hot rolling process while high difusibility interstitial carbon composition tends to even out in the as-rolled structure. Manganese, present in all samples at $0.44 \leq \%Mn \leq 0.74$, lowers Ar_3, stabilizing austenite so that while in low-manganese regions, austenite transforms to pro-eutectoid ferrite forming ferrite bands. In manganese-rich regions, the carbon from the low Mn regions combines with ferrite at a lower temperature to form pearlite bands (Krauss, 2003). Banding tends to marginalize strength characteristics. Thus sample P20 with the microstructure in Fig.4.7 shows a higher σ_u/τ_{max} (Table 4.3) than all steels of similar carbon content. This is an indication of stronger longitudinal than radial properties in spite of the self-annealing effect of hot rolling.

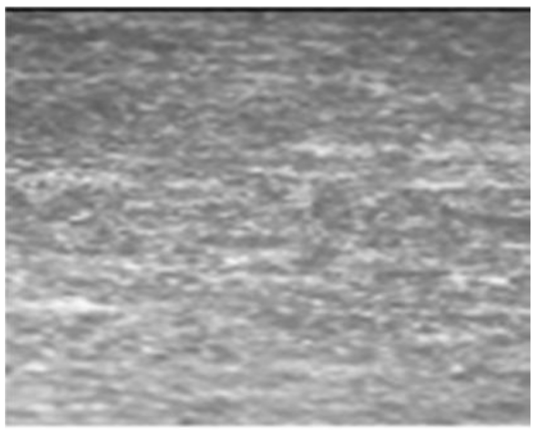

Fig 4.3: Banding in sample P20

Many samples showed varying microstructures when analyzed at different positions along the length of the bars in response to similar disparity in composition as seen earlier. Some samples for example analyzed at longitudinal intervals indicate a microstructure with substantial post hot rolling faults. Fig.4.8 for example, shows a transverse section of P2 revealing a large inclusion. By virtue of its relative dimensions and chemical distinction from the surrounding metallic material, this is a non-metallic, exogenous inclusion. Such inclusions are usually due to the entrapment of refractory materials such as induction furnace lining (Atkinson *et al,* 2002). Induction furnaces are typically used in steel recycling in this country.

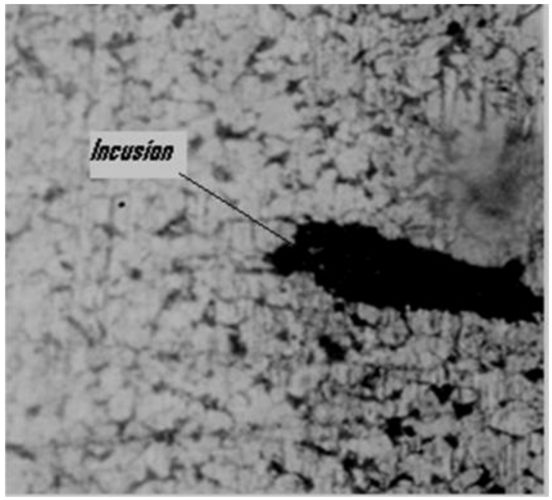

Fig 4. 4: Non-metallic inclusion in P2

Failure of steel components actually starts from larger inclusions (Cogne *et al*, 1986). Non-metallic inclusions in a steel matrix are known to be the main cause of fatigue and tensile crack nucleation (Grigorovich *et al*, 2010). Owing to their low thermal coefficient, such inclusions create tensile stresses during the solidification process that can approach yield strength of the matrix in which they are interposed and given their sharp edged contours, result in micro-cracks. These cracks nucleate more easily if the inclusion particle is rigid, has low cohesion with the matrix, or has low internal fracture strength. Hard and brittle inclusions like refractories tend to provoke de-cohesion at the inclusion-matrix interface at negligibly small strains (Yousef *et al*, 2007). The inconsistent nature of many of the portions of the same bar is the result of such inclusions giving rise to erratic fractures.

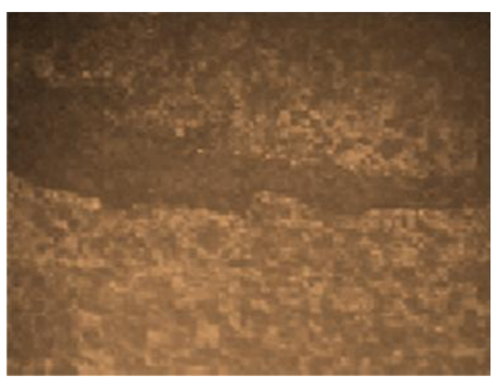

Fig 4. 5: Lap in sample T30

In Fig. 4.9, sample T30 showed a typical lap, consisting of oxides covered by folding over of material due to misalignment of the pass lines or rolls. Damaged or poorly set rolls are the major factors leading to laps on hot rolling (Newby *et al*, 1989). Irregular strength and hardness properties in which stronger, harder steel portions pass where setting was done for softer steel destabilize roll setting and cause misalignment and damage to roll grooves and profiles. Tramp elements, being a common source of irregularities in steel properties as indicated earlier are the major factor in the generation of laps in steel bar surfaces. During reheating which is the solution treatment meant to allow the dissolution and diffusion of solute precipitates in austenite phase, the final rolling temperature and soaking time needed for homogenization are set as a function of the carbon equivalent (Daramola *et al*, 2010). In reality its value changes along the length of the bar, causing varying austenite strengths. Besides their effect on tensile strength of hot rolled steel, laps reduce shear strength. Table 4.3 shows values of the ratio of tensile to shear stress, σ_u/τ_{max} for T30 as one of the highest in spite of having one of the lowest tensile strength values in Table 4.2(b).

4.2.3 Mechanical and Geometrical Properties

The force-elongation curves for all the samples showed ductile type of material, some with a reasonable yield platform indicating a clear yield processes as in sample T1 shown in Fig.4.10. The values of the ratio of maximum stress to yield ranging from 1.56 to 1.78 for P series and 1.37 to 1.49 for T series in Table 4.2(a) and 4.2(b) respectively, further emphasize ductility.

The samples in group T show larger ductility ranges (permanent deformation) due to generally less carbon and manganese content (Table 4.1b). There were however large differences between values of yield and maximum stress shown by different sides of the same samples due to marked differences in composition and structure (Table 4.4) as shown earlier.

The elevated values of ultimate and yield stresses as seen Table 4.2(a) and (b) are due to the relatively high carbon and manganese content. These lay between $0.23 \leq \%C \leq 0.51$ for P series and $0.24 \leq \%C \leq 0.51$ for T series and $0.45 \leq \%Mn \leq 0.74$ for the P series and $0.44 \leq \%Mn \leq 0.67$ for the T series respectively as in Table 4.1(a) and (b) and are reminiscent of their recycled origin and the consequent difficulty in closely controlling their composition with the available technology.

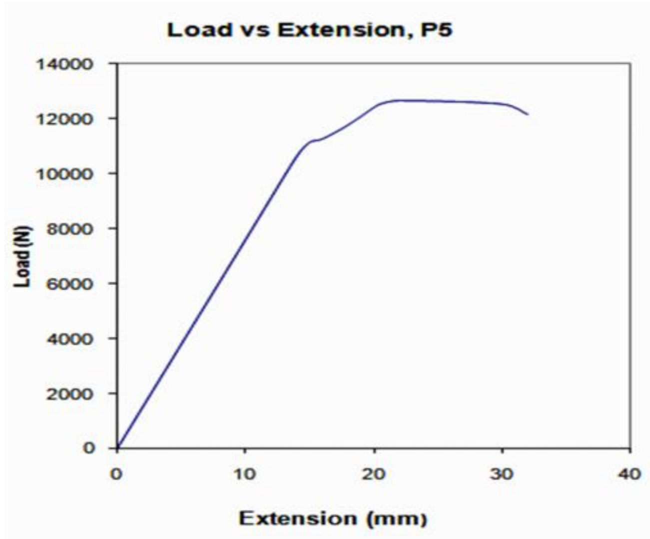

Fig 4. 6: Load Extension Diagram for Sample T1

These correspondingly engender the wide variation in the yield and ultimate strengths whose high values fluctuate from sample to sample quite amply 531≤σ_u (MPa)≤647 for P series and 422 ≤σ_u (MPa)≤ 663 for T series. The same recycled origin factor determines the scatter of the otherwise high percentage elongation (ductility) values characterizing both groups at 14≤ δ% ≤28 for the P series and 17≤ δ% ≤42 for T series.

At normal reheating temperatures (between 1000°C and 1200°C), there is a tendency for surface oxidation to occur. The preferential oxidation of iron, leaving inoxidisable copper on the steel surface permits high copper concentrations and the formation of copper based phases. Copper tends to penetrate austenite grain boundaries in this form at these elevated temperatures, resulting in grain boundary incoherence and hot-shortness during rolling (Savov *et al*, 2003). It is, however, also true that the solubility of copper in austenite is increased with temperature, reducing the availability of liquid copper (Christian, 2007). These two conflicting positions reach a compromise for reheating temperatures of 1200°C for steel with copper composition up to 0.39%Cu above which no tendency to crack is observed in copper bearing steel (Garza *et al*, 2005). Copper dissolved in austenite tends to cause grain refinement, resulting in higher end product ductility and strength, (Olivier *et al*, 2006). The samples studied returned 0.34≤%Cu≤0.45 for the P series and 0.34≤%Cu≤0.42 for the T series. The copper content here contributes strongly towards the relatively high ductility of the steel. The use of prolonged re-heating holding times which tends to lead to the consumption of metal by oxidation, hence getting rid of pre-existing copper induced surface defects also enhances the tendency to high ductility values.

The maximum shear stress for the bars in T-series stood at 245≤ τ_{max}≤431 MN/m^2 while those of P-series were 398≤τ_{max}≤503, MN/m^2. All the samples reached the τ_{max}=245MN/m^2 mark.

All the bars without exception had very low dimensional consistency and were substantially underweight according to the East African Standard EAS 412-2:2005 admissible ±5%. The cross section area varied by between 18 and 24% from the normal size as shown in Tables 4.2(a) and 4.2(b). This shows that not enough allowance has been made for solidification shrinkage and surface oxidation during projections for the initial roll setting.

4.3 Reinforcement With Twisted Bars

Table 4.7 shows the mechanical properties of five samples analyzed in Paper 3. The values of the yield stress were quite high for grade RB 460 according to EAS 412-1:2005, TS1 returning the smallest at 520Mpa. The corresponding values for tensile stress were similarly elevated. The calculated values of σ_u/σ_y range between 1.06 and 1.13, indicating a substantial strain hardening range and apart from TS1 which returned 11% elongation, the rest of the samples are sufficiently ductile, ranging between 14 and 21%.

Table 4.7: Mechanical Properties of Twisted Bars

Sample	σ_U	σ_y	σ_U/σ_Y	*δ%*
TS1	573	520	1.11	11
TS2	613	580	1.06	16
TS3	653	584	1.12	18
TS4	648	574	1.13	21
TS6	645	587	1.10	14

Table 4.7 shows the composition of the five samples. Their carbon content, being on the lower range, was between 0.16 and 0.22. The phophorous and sulphur levels were appreciably low, being between 0.020 and 0.31. This is in addition to the low manganese levels at 0.46≤ Mn%≤ 0.60 compared to the allowable 1.6%Mn.

Comparing the values in Table 4.7 with the standard requirements of the EAS 412-2:2005 (ISO 6892), it is evident that the yield stress of the steel bars was quite high. It is often believed that the higher the strength of the reinforcement bars, the better they are. This is not true and is in fact largely self-defeating.

The purpose of reinforcing concrete with steel bars is to impose a degree of ductility and tensile strength not attainable with concrete alone. Ductility depicts the ability of a member to survive large deformations; absorbing energy in the process by hysteretic behavior. When steel bars are cast together with concrete to form reinforced-concrete, it is understood that at the time of plastic deformation, the concrete-steel compound structure should be able to deflect together. This actually means that the yield stress of the steel bars which will mainly be experiencing tensile and compressive stresses when the beam is bending must occur at that crucial moment when extensive deformation commences.

Within the yield plateau, a substantial amount of energy is absorbed without further increase in stress, allowing ample warning of the impending structural failure. This is extremely desirable especially as in many cases; this yield point elongation is visually noticeable and is the actual opposite of fragile failure being prevented by the concrete reinforcement in the first place. In general, the forces that could be developed in a structure during the process of failure decrease with increasing ductility owing to energy absorption (Xu Youlin , 2010). The energy absorption capacity of the fracture is ultimately the real indicator of the ductility inducing effectiveness of steel bars.

Noteworthy too, is that the strain hardening zone that follows the yield-platform as stress increases tends to render the reinforcing bars stiffer by increasing yield stress by up to 40% through strain hardening. Ductility reduces simultaneously (Tian *et al*, 2010).

Basically all tramp elements contribute to an increase in strength and the associated ductility loss. These effects are more pronounced for low carbon steels than for medium and high carbon steel grades (Janke *et al*, 2000). The difficulty in controlling the tramp element content of steel in the induction furnace process in Uganda, therefore, gives rise to the production of steel of relatively high yield and tensile stresses even though research has shown that the values of tensile to yield stresses are averagely acceptable (Senfuka *et al*, 2012).

The addition of atoms of elements that occupy interstitial or substitutional positions in parent iron (steel) lattice increases the strength of parent material by solid solution strengthening, dispersion strengthening, solute drag effect and grain size control. Several of these elements are frequently present in recycled steel and are additive in their effect, increasing the yield point the more the quantities of the elements are present (equation 2.7).

The non-spherical distortions, known to be caused by most interstitial atoms, have a strong strengthening effect per unit concentration amounting about three times their shear modulus. Conversely, spherical distortion caused by substitutional solute atoms has a relatively smaller strengthening effect being of the order of a tenth of their shear modulus. The strengthening achieved by substitutional solute atoms is, in general, greater the larger the difference in atomic size of the solute from that of iron (Fe) subject to the Hume-Rothery size effect (Satish, 2009).

Table 4. 8: Chemical Composition of Twisted Bars

	TS1:16mm	TS2:16mm	TS3:10mm	TS4:10mm	TS6:20mm
C	0.16	0.17	0.19	0.22	0.22
Si	0.20	0.17	0.20	0.17	0.27
Mn	0.56	0.54	0.46	0.49	0.60
P	0.031	0.031	0.023	0.020	0.027
S	0.042	0.037	0.033	0.03	0.035
Cr	0.11	0.10	0.09	0.07	0.12
Mo	0.010	0.009	0.010	0.009	0.008
Ni	0.15	0.13	0.12	0.11	0.12
Al	0.040	0.02	0.012	0.016	0.002
Cu	0.20	0.16	0.16	0.20	0.23
As	0.0150	0.0132	0.0280	0.0165	0.0175
Sn	0.031	0.054	0.048	0.030	0.051
V	0.002	0.003	0.001	0.003	0.001
Nb	0.003	0.001	0.001	0.001	0.010
B	0.0016	0.0021	0.0021	0.0013	0.0024
Co	0.001	0.006	0.005	0.003	0.004

Thus the presence of manganese (Mn), silicate (Si), vanadium (V), niobium (Nb), nickel, molybdenum and a host of other substitutional elements in the steels in this study (Table 4.4), while increasing the strength of the steel, has had a smaller total effect than that of interstitial elements like Boron present in smaller percentages and numbers.

Additionally, the hardenability of steel, for example, resulting in the thermal mechanical elevation of the yield point, is known to be increased by the presence of small dissolved amounts of boron in steel in the range of 0.001 to 0.003.

This is caused by the precipitation of iron boron carbide, $Fe_{23}(C,B)_6$, at the austenite boundaries during cooling from the fully austenised condition either during billet solidification on casting or during the rolling process, retarding the transformation of austenite to ferrite by impeding the nucleation of ferrite and other soft structures. The effect of boron is higher the lower the carbon content (Murali *et al*., 2011). The boron content in this case is in the range 0.0013 to 0.0024 (13ppm to 24ppm). The carbon content is well in the lower range ($0.16 \leq \% \leq 0.22$).

On the other hand tin (Sn), originating from the tin coating on steel packaging, although not effective in small quantities like 0.03%, actually increases the yield stress of steel by up to 20% when increased to 0.08% .

The tin content in TS2 and TS3 and TS6 ($0.048 \leq S\% 0.058$) here is in consonance with the high yield they returned. Arsenic, equally present in all the five steel samples is much less effective in increasing the steel yield point.

Many of the steels in this study showed a reasonable yield platform. This has been shown earlier to be very important in the effectiveness of steel as concrete reinforcement. The occurrence of the yield point phenomenon itself is associated with presence of small amounts of interstitial or substitutional impurities. This is so because either unlocking of dislocations by a high stress for the case of strong pinning or generation of new dislocations are the reasons for yield-point phenomenon (Satish, 2009). It is non-the-less true that the existence of these same elements in the form of residual elements gives rise to the elevation of the yield value.

4.4 Weldability of Steel Bars

Out of the thirty pieces prepared and welded in Paper 4, four samples: PV5, PV8, PV19 and PV26 returned weld cracks. The chemical composition of the four samples which developed cracks were as in Table 4.9. The four samples have carbon content levels falling in the range $0.22 \leq C\% \leq 0.27$. The Manganese content is also medium. Worth noting is the presence of Boron at $0.002 \leq B\% \leq 0.004$. The Chromium, Nickel and Carbon equivalents were as in Table 4.8 as determined by equations 3.1, 3.2 and 3.3

Table 4. 9: Chemical Composition of Welded Bars

S'ple	%C	%Cu	%B	%Ni	%Cr	%Mn	%Mo	%V	%Si	%Nb	%Ti	%Al	%W	%Co
PV5	0.24	0.364	0.004	0.062	0.544	0.483	0.115	0.0025	0.062	0.032	0.0005	0.030	0.01	0.004
PV8	0.25	0.217	0.003	0.051	0.251	0.527	0.113	0.0005	0.051	0.033	0.0005	0.021	0.01	0.007
PV19	0.27	0.321	0.004	0.100	0.153	0.582	0.013	0.0030	0.247	0.001	0.0010	0.036	0.01	0.006
PV26	0.22	0.354	0.002	0.062	0.373	0.499	0.110	0.0005	0.054	0.034	0.0005	0.039	0.01	0.004

The micro-hardness plotting across the face of the samples PV5 and PV19 is shown in Fig. 4.13 and 4.14 respectively. The hardness value at the centre of PV5 gradually drops ten HRb units below that of the base metal in response to the lower carbon equivalent of the filler rod (See Table 4.11) in the center in comparison to the edges. The final five units drop in hardness is in the center of the sample, showing the position of the crack.

In the case of PV19, the micro hardness plot indicates the expected reduction in hardness in the weld fusion zone but suddenly drops 30 HRb units towards the right edge of the sample. The crack is located outside the weld and is well inside the parent metal. This is reflected in the photographic representation of the surfaces of PV5 and PV19 treated with a red dye penetrant and developer in Fig.4.11 and 4.12.

The presence of crack promoting elements like Boron, Chromium etc in the HAZ makes weld cracks a likely occurrence. In the empirical relationship for carbon equivalent in equation 3.3, the effect of carbon and boron is strongly shown to favor welding crack formation.

Table 4.10: Chemical Equivalents

S'ple	Ni_{eq}	Cr_{eq}	C_{eq}
PV5	7.62	1.08	0.54
PV8	7.89	0.71	0.49
PV19	8.59	0.89	0.49
PV26	7.02	0.93	0.48

These elements tend to elevate the carbon equivalent value and the critical cooling rate which in turn determine the crack forming susceptibility of the microstructure and thus increase the hydrogen cracking tendency. The boron content in PV5 and PV19 at 0.004 is relatively higher than the rest of the samples tested (Table 4.9).

Table 4.11: Deposited Metal Composition

Element	C	Mn	Si	S	P
% Comp.	0.12	0.05	0.35	0.035	0.04

Fig. 4. 7: Cold Cracking, PV19

Fig. 4. 8: Centerline Crack in PV5

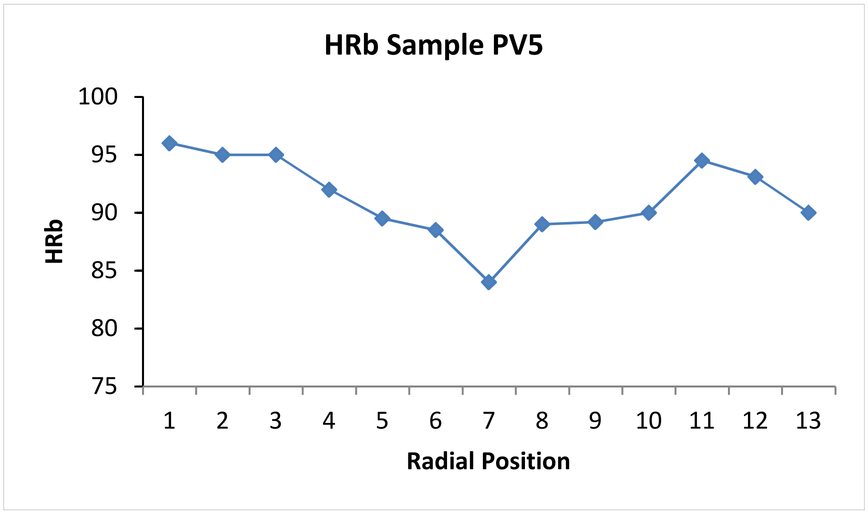

Fig 4. 9: Micro-hardness Plot for PV5

There have also been suggestions regarding effects of pre-existence of defects like inclusions, minor phase particles, microscopic cracks, and other discontinuities acting as initiation sites in hydrogen initiated cracking (Devletian *et al*, 2008). The presence of large amounts of tramp elements in recycled steel and specifically the four samples in Table 4.9 invariably leads to multitudes of minor phase particles in their different forms such as MnS, Cr_7C_3, WC etc. This also includes products of deoxidation like Al_2O_3.

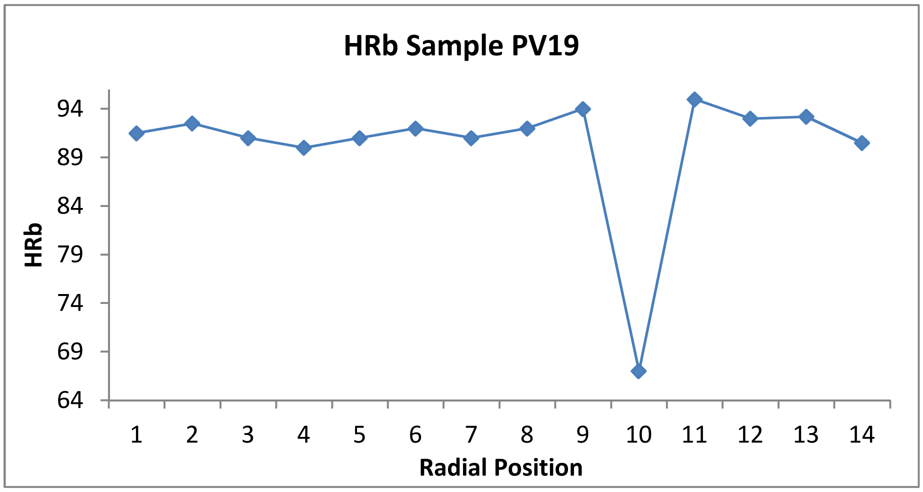

Fig 4.10: Micro-hardness Plot for PV19

It has also been argued that during the welding process, while the metal is still in molten state, molecular hydrogen dissolves readily in the molten metal, but dissociates once in solution and is retained as a mono-atomic solute and upon solidification. As an interstitial solute, mono-atomic hydrogen is relatively mobile, even at ambient temperatures. However, due to lattice imperfections in the crystalline structure, the interstitial atom cannot be maintained with this mobility. These lattice defects present areas where the lattice strain induced by the solute hydrogen atom is reduced, tending to act as hydrogen traps. Once trapped, the hydrogen atom, although still as single atom, becomes relatively immobile. If, as is normally more likely to be the case, the trap is a line defect, there will accumulate a string of hydrogen atoms along the defect. The presence of a string of individual hydrogen atoms would increase the force needed to cause deformation. This would even be the more so if two adjacent atoms on a line defect recombine to form molecular hydrogen (Carter *et al*, 2001). The applied stress required to cause movement thus becomes much greater, effectively pinning the dislocation at that point and since dislocation movement is the underlying process to plastic flow, the ductility of the material is reduced and the probability of brittle failure increased by the presence of hydrogen. Interfaces such as grain boundaries or second phases act as dislocation arrays which are likely to accumulate solute hydrogen, quite possibly in molecular form, embrittling the interface. The presence of large multitudes of tramp elements in recycled steel in Uganda gives rise to many chances of second phases and particulates. Lattice defects are also more likely in steels with many solute components. It may be pointed out that the base metal, with so many solutes (tramp elements) as shown in Table 4.9, provides one of the essential conditions for cold crack formation and propagation: the crack sensitivity of the microstructure.

The HAZ, affected by the welding arc, is transformed from the room temperature structure of ferrite to high temperature austenite. The subsequent cooling of the metal will convert to structures resulting directly from the carbon and alloy (tramp) element content which will determine the carbon equivalent, and hence the hardenability of the steel and the cracking sensitivity. The higher the carbon equivalent value, the greater the risk of hydrogen cracking. Steels with a carbon equivalent value of less than 0.4 are not susceptible to HAZ hydrogen cracking as long as low hydrogen welding consumables or processes are used (Bailey *et al*, 2004).

All steels in this study have carbon equivalent above this limit although they are not particularly high in carbon content (Tables 4.9 and 4.10). This means that the overall tramp element content is the major factor behind this elevated carbon equivalent value. The corresponding position on the Schaeffler diagram drawn from Table 4.10 for the four steels is as shown in Fig.4.15. It can be seen from this diagram that the tendency to formation of martensite and other non-equilibrium products is substantial. This provides ideal conditions for cold (hydrogen) cracking which then only depends on the weld design.

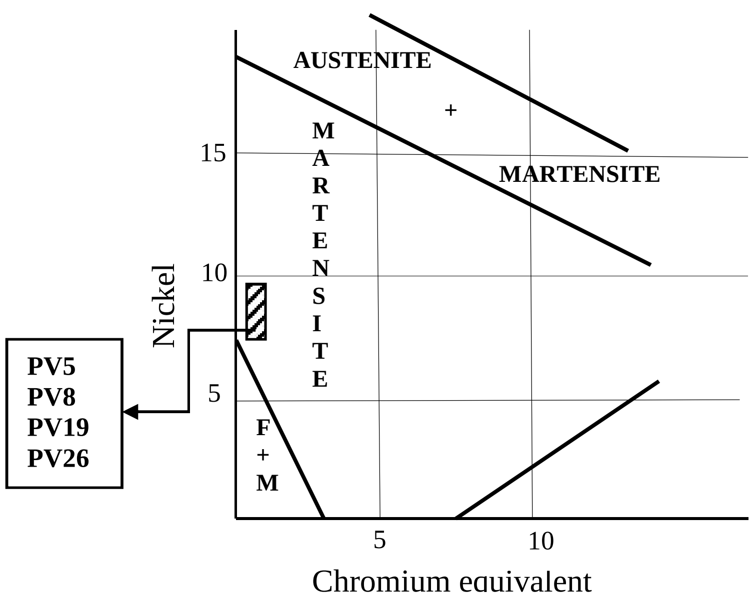

Fig 4.11: Scheafler Diagram for PV5, PV8, PV19, PV26

4.5 Thermo-Mechanically Treated Bars

Paper 5 scrutinizes thermo-mechanically treated bars and the results are presented here.

The comparison of maximum and minimum hardness between extreme ends A and B of the bars and the minimum and maximum micro-hardness values across the sections of the bars are shown in Table 4.12. The maximum hardness corresponding to the martensite ring stands out clearly while the demonstrably softer ferrite/pearlite forms the core in each case giving the bars their characteristic resilience.

Four outstanding micro-hardness plots are shown graphically in Fig.4.16, 4.17, 4.18 and 4.19. Their average chemical composition and carbon equivalents were as in Table 4.13.

Table 4.12: Comparative Hardness Values (HRc)

Sample	Min	Max	Max/Min
R1(A)	9.8	30.2	3.1
R1(B)	8.6	29.6	3.4
R7(A)	12.7	28.2	2.2
R7(B)	5.7	26.4	4.6
R16(A)	2.4	25.0	10.4
R16(B)	2.8	24.0	8.6
R22(A)	18.0	30.5	1.7
R22(B)	18.5	26.5	1.4
R27(A)	19.2	28.9	1.5
R27(B)	17.2	28.0	1.6

Table 4.13: Average Composition of TMT Bars

Sample	C	Cu	Mn	Cr	Ni	Si	Ti	Mo	Nb	B	V	C_{eq}
R1	0.207	0.04	0.60	0.07	0.126	0.247	0.001	0.008	0.001	0.0009	0.009	0.35
R7A	0.197	0.04	0.60	0.07	0.128	0.245	0.001	0.008	0.001	0.0010	0.009	0.34
R7B	0.191	0.04	0.42	0.07	0.125	0.144	0.001	0.008	0.001	0.0004	0.009	0.29
R16	0.195	0.11	0.60	0.05	0.043	0.271	0.001	0.014	0.001	0.0010	0.003	0.33
R22	0.202	0.13	1.15	0.06	0.061	0.409	0.001	0.025	0.001	0.0014	0.004	0.44

That the micro-hardness readings of R4, R13 and R22 on both sides of the bars, however, showed very low outer ring-to-core hardness ratio as demonstrated by the micro-hardness plot for R22 in Fig.4.19 and the maximum to minimum hardness in Table 4.12 is a symptom of low equalization temperature which resulted from the steel from one part of the teeming ladle having had a different composition from the average one determined prior to the setting of the spray nozzles. This is known to happen as a result of the difference in composition of the different scrap types melted in the induction furnace, leading of unequal composition of the final melt.

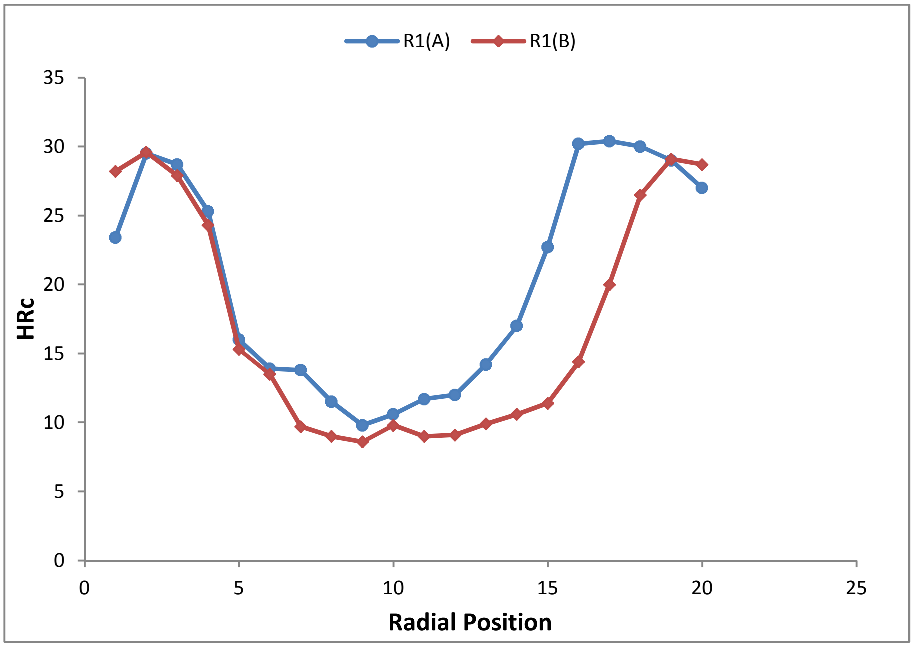

Fig 4. 12: Micro-hardness Plot for R1

Lack of stirring action at the teeming ladle stage makes one part of the melt to have both different composition and temperature from the other parts (Nordstrand, 2009). The composition of R22 in Table 4.13 was only slightly high carbon content but had a relatively elevated manganese and silicon content with an accompanying high carbon equivalent (0.44).

The hardness obtained after tempering (tempered martensite) is a linear function of the original hardness after quenching which in turn is determined by the carbon content (Suksai, 2007) and the alloy/tramp element content (Poursaeidi, 2008).

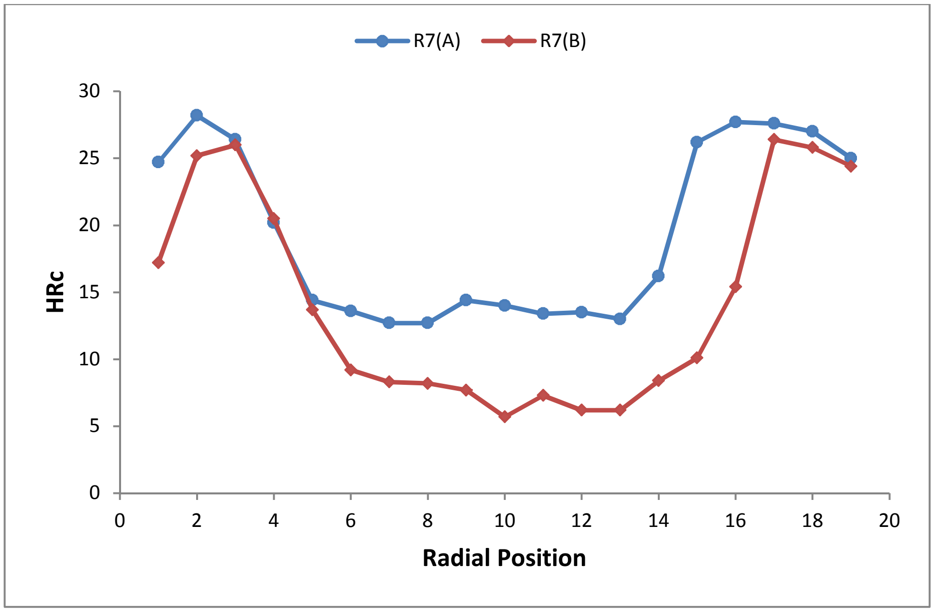

Fig 4. 13: Micro-hardness Plot for R7

The tramp elements have individual effects that are additive and increase with particular alloying element content (Grange *et al*, 1977). This is summarized in equation (4.1) (Spies, 1992):

$$HB = 2.84H_h + 75(\%C) - 0.75(\%Si) + 14.25(\%Mn) + 14.77(\%Cr) + 128.22(\%Mo) - 54(\%V) - 0.55(T_t) + 435.66 \ldots.(4.1)$$

where *HB* is the hardness after hardening and tempering, H_h the hardness after quenching and T_t the hardening temperature.

The tramp element content uplifts the steel carbon equivalent so that the steel hardenability (critical diameter) which gives rise to more martensite at the core would have required a higher equalization temperature than the one set for the average composition of the steel. This would be in order to give the conversion of the carbides time to dissolve and facilitate the conversion of martensite to softer, more ductile pearlite to facilitate the formation of the combination of hardness at the surface and toughness at the core characteristic of TMT bars. Additionally, almost all alloying /tramp elements in steel (with the exception of cobalt) tend to reduce M_s and M_f temperatures, making it easier for martensite to form deeper in the section and at lower temperatures with increasing dislocation density in the martensite. Alloying elements also reduce the critical cooling rate with a similar effect (Chong, 2008).

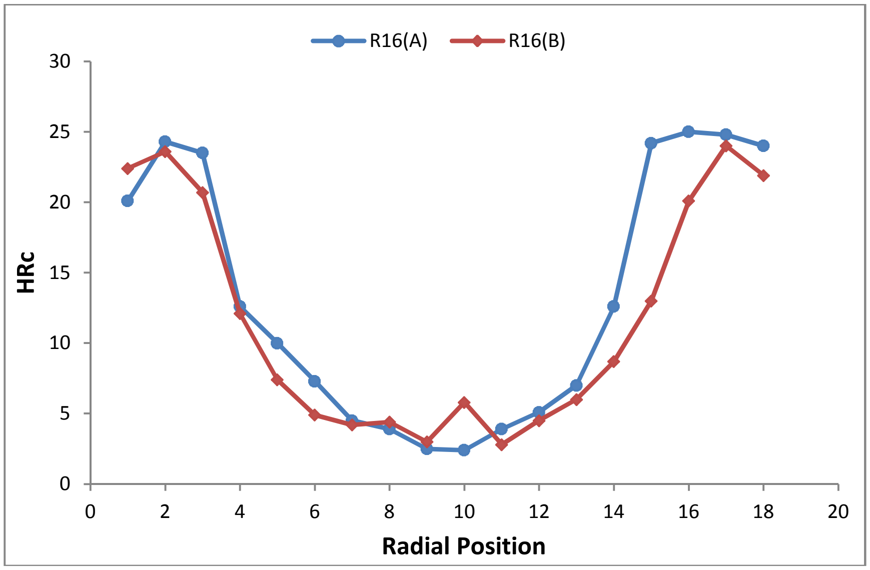

Fig 4.14: Micro-hardness Plot for R16

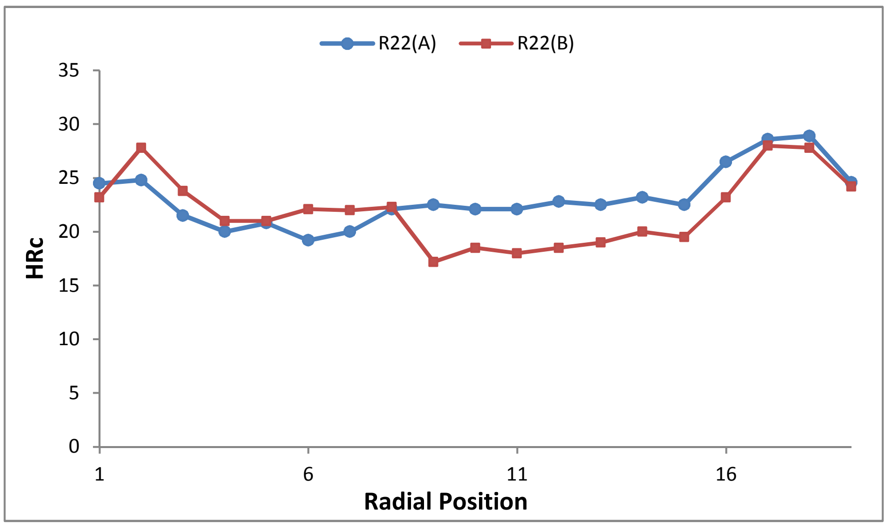

Fig 4. 15: Micro-hardness Plot for R22

R7 and R16 (Table 4.12) also show a wide difference in the micro-hardness between one extreme and the other. For presumably the same quenching conditions and equalizing temperature, the only possible reason is variation in composition between end A and end B, leading to different critical diameters (hardenability). This is reminiscent of the recycled origin of the steel bars and their tramp element content (Senfuka et. al., 2012). An examination of the composition of the ends of R7 is in Table 4.12. Important strengthening elements like Boron, silicon and manganese vary substantially between the two extremes leading to lower hardenability for end B than end A.

R7 is an example of the asymmetry in properties in some bars which repeats itself to an extent in R1 (Fig.4.17) and R16 (Fig.4.18). While this could be due to unequal quenching and/or tempering conditions, the more likely cause would be variation in composition across the diameter equally the result of unequal distribution of tramp elements across the relatively large diameter of the bars, resulting in differences in hardenability.

Prior to the making of TMT bars, the composition of the steel is determined and the optimum cooling conditions set to guarantee that the maximum temperature attained at the surface of the bar after quenching (the equalization temperature), which will be the tempering temperature for that composition, gives a resulting steel bar with the correct ratios of volume and hardness of the tempered outer ring to the pearlite/ferrite core (Mukhopadhyay *et al*., 2011). These cooling conditions include the final billet rolling temperature which represents the quenching temperature, spray intensity and billet speed at the final roll (Bhupinder *et al*, 2002).

The fact that samples R16, R21, R23, R25 and R26 have almost ideal micro-hardness distribution with moderate composition in terms of carbon, manganese and other elements leading to equally moderate carbon equivalent values as exemplified by R16 in Fig.4.18 and Tables 4.12 and 4.13 therefore shows that the equalization temperature corresponded with that required for the respective steel compositions.

That the micro-hardness readings of R4, R13 and R22 on both sides of the bars, however, showed very low outer ring to core hardness ratio as demonstrated by the micro-hardness plot for R22 in Fig.4.19 and the maximum to minimum hardness in Table 4.12 is a symptom of low equalization temperature which resulted from the steel from one part of the teeming ladle having had a different composition from the average one determined prior to the setting of the spray nozzles. This is known to happen as a result of the difference in composition of the different scrap types melted in the induction furnace, leading of unequal composition of the final melt. Lack of stirring action at the teeming ladle stage makes one part of the melt to have both different composition and temperature from the other parts (Nordstrand, 2009). The composition of R22 in Table 4.13 was only slightly high carbon content but had a relatively elevated manganese and silicon content with an accompanying high carbon equivalent (0.44). The hardness obtained after tempering (tempered martensite) is a linear function of the original hardness after quenching which in turn is determined by the carbon content (Suksai, 2007) and the alloy/tramp element content (Poursaeidi, 2008). The tramp elements have individual effects that are additive and increase with particular alloying element content (Spies, 1992).

Finally and of great importance is that all the samples met the strength and ductility requirements as depicted by the σ_u and the (σ_u/ σ_y) ratio. This actually shows that on the whole, the unequal properties kept within the standard values in accordance to EAS 412-2:2005.

4.6 Steel Reinforcement Value and Tramp Element Content

Table 4.12 shows the yield values of the 72 thermo-mechanically treated bars. The chemical composition for bars with σ_y> 550Mpa was as displayed in Table 4.13.

Table 4.14: Steel Yield (Mpa)

469	497	504	515	523	528	531	534	537	542	551	555
477	499	506	515	523	528	532	535	537	543	551	560
488	501	508	516	524	529	532	536	537	546	551	572
488	502	509	517	525	530	533	537	539	548	552	576
490	502	510	521	526	530	533	537	540	549	552	584
491	502	514	522	528	531	533	537	541	550	553	588

Figure 4.20 shows an Excel spreadsheet plot of the steel yield values against their respective frequencies of occurrence. The bell shape largely conforms to the Normal Distribution Function with mean value of 528 Mpa and standard deviation 22.5.

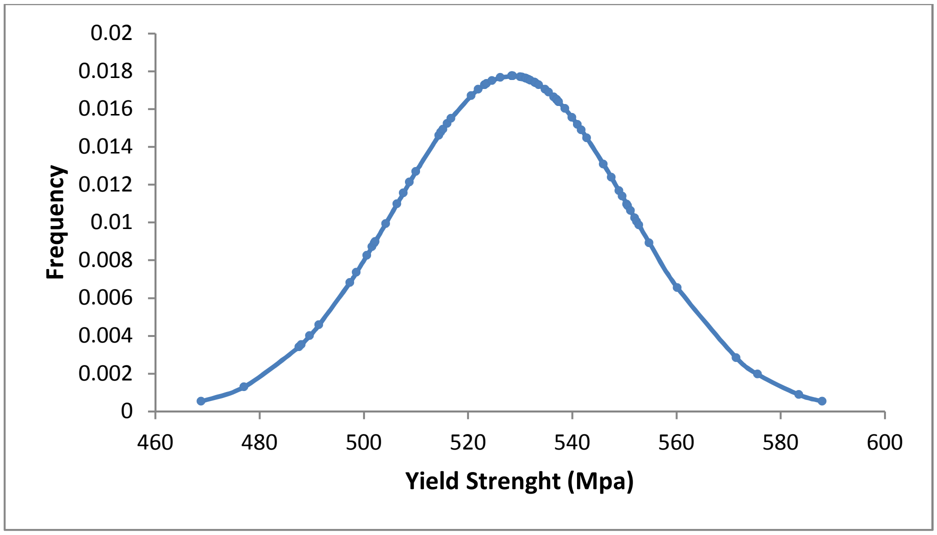

Fig 4. 16: Frequency Distribution of Yield Stress

The standard score $z = (\chi - \mu)/\sigma$ calculated as (550-528)/22.5 yields 0.977 which from the standard normal distribution table gives to $P(X \geq \chi) = 1 - P(X \leq \chi) = 0.22$ or 22%. Thus up to 22 percent of the recycled steel samples gave above the design yield stress value.

In Table 4.14, the composition of the bars with yield stresses of 550Mpa and above along with the corresponding Boron, Molybdenum and Vanadium content are shown. Vanadium at 0.04% would have a hardenability factor of less than 1.1(Fig. 2.9) and is there for not substantial. Both manganese and chromium affect the Ms value by less than 10°C (Fig.2.10) and are therefore not the source of the variation in hardenability. The fact that Niobium and Titanium, whose main effect would result from grain size reduction, are present at extremely low levels, both being below 0.001% indicates that their grain size effect was not reached (Fig.2.11). The Nitrogen content was also below significant level.

Table 4. 15: Yield Strength and Composition of Bars above 550Mpa

σ_y	B	Mo	V	σ_y	B	Mo	V
550	0.0020	0.0210	0.0010	553	0.0015	0.0210	0.0010
551	0.0026	0.0203	0.0013	560	0.0018	0.0200	0.0013
551	0.0008	0.0201	0.0012	572	0.0006	0.0198	0.0010
551	0.0014	0.0207	0.0011	576	0.0021	0.021	0.0010
552	0.0022	0.0214	0.0013	584	0.0022	0.0215	0.0021
552	0.0018	0.0240	0.0010	588	0.0027	0.0019	0.0010
558	0.0018	0.0184	0.0015	555	0.0010	0.0201	0.0008

Additionally, a plot of yield strength against the Carbon, Manganese and Boron content was as in Fig. 4.21. The % Boron-Yield curve has been extracted in Fig.4.22 for clarity and shows the marked effect on hardness of Boron relative to expected key players, carbon and manganese.

Thermo-Mechanically Treated (TMT) steel bars have been developed to provide yield values of 500 to 550Mpa for longitudinal reinforcement (ACI 318-08, 2008). The consistent tallying of the steel yield values with the normal distribution function and therefore satisfaction of the normal equation $Y = \frac{1}{\sigma\sqrt{(2\pi)}} e^{-\frac{(x-\mu)^2}{2\sigma^2}}$ as the probability density function enables the determination of basic statistical functions and several important factors in the reinforcement function of the bars.

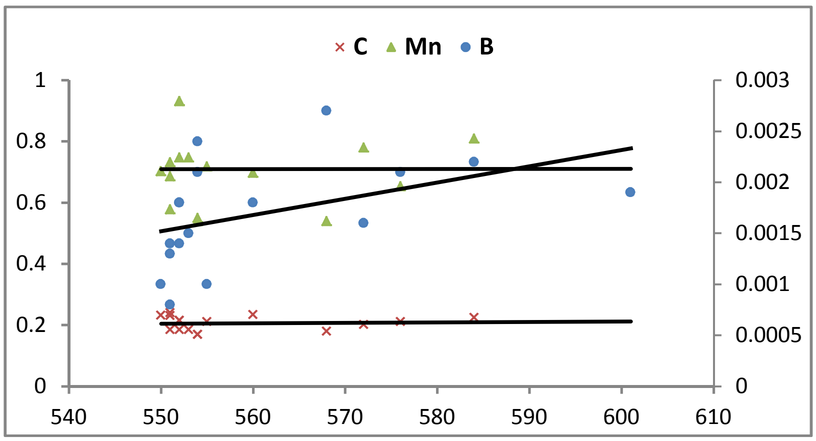

Fig. 4.17: Plot of C, Mn and Boron Content against Yield

The samples in this study show that a large portion of these bars will be well above 550Mpa and the development length based on these values will not be the weaker part of the chain as required. Equation 2.14 shows that if in σ_y/τ_c, the value τ_c is held constant; since the concrete type is preselected as mentioned earlier, the development length l_d will be directly proportional to the yield stress σ_y and has a similar distribution. This is also in conformity with the American Concrete Institute (ACI) development length in equation *iv)* ACI 318-08, equation 12-1. Fig. 4.21 and Fig.4.22 show the dependence of the growing yield on mainly the Boron content which fluctuates between 0.0006 and 0.003. All these steels are aluminium killed, guaranteeing reduced tendency to formation of boron oxide (B_2O_3) and Boron nitride (BN) even though the nitrogen fixers, Titanium and Zirconium are very low content in all cases. The Boron to Nitrogen (B/N) ratio is also substantial and certainly well over the stoichiometric value since the Nitrogen content in all cases is negligible. Taking into account the effect of carbon on the Boron factor

(Fig.2.8), the carbon content in most of the TMT bars is below 0.25. Small amounts of Boron remarkably increase the hardenability of low alloy steels. Furnace linings contain boric acid (H_3BO_3) added to improve the sintering process of the high alumina and silica refractory lining materials which on exposure to heat, forms boron trioxide, B_2O_3. The Boron oxide is reduced by carbon at high temperature and boron is dissolved in the liquid iron (Haley, 2012). The Boron that is free of oxygen and nitrogen reduces ferrite nucleation, slows the diffusivity of carbon, reduces the number of nucleation sites and can precipitate as a complex carbide as discussed earlier. The higher Boron content in the steels above the 550MPa mark is therefore responsible for the raised yield level in these samples.

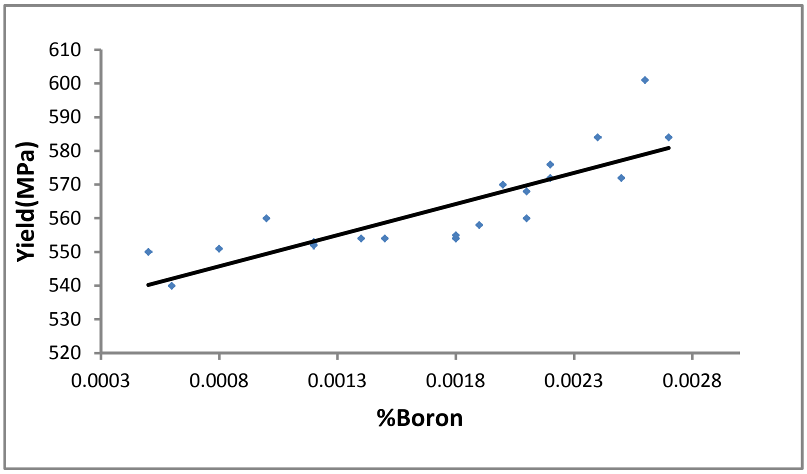

Fig 4. 18: Yield against Boron Content

CHAPTER FIVE: CONCLUSIONS AND RECOMMENDATIONS

5.1 Conclusions

5.1.1 State of the Industry

Mini mills especially using the induction furnace alternative are the most widely used and suitable steel mill type in Uganda. This is mainly due to their less capital intensive nature, easier installation, resilience, low fixed asset to total assets ratio as well as low skills requirements. The possibility of introducing direct reduced iron (DRI) as sweetener given the availability of iron ore and discovery of natural gas reductant strengthens the future of the otherwise depleting scrap steel resources as row material. The technology currently in use encourages small plants. This is preferred to the more extensive sponge iron making processes such as the Midrex used in Trinidad and Tobago producing at 1.2 million tons per annum because of the reduced state involvement and minimal investor capital base.

5.1.2 General Properties of the Steel

The steel in the present study was largely acceptable in metallurgical and mechanical values in spite of the elevated carbon and manganese content as seen in Paper 2. The issue however is that even inside the prescribed standard bracket of composition, the manganese content varies so widely amongst the samples that the quality of the resulting steel cannot be said to be predictable. Many of these steel bars have excellent properties in some parts but because of inclusions and uneven elemental distribution, display sudden changes owing to the erratic nature occurrence of inclusion and residual elements since ductile fracture in steel is caused by the nucleation, growth, and coalescence of voids which are nucleated at hard particles such as inclusions, pearlite nodules etc. Their distribution in the steel bars even for a given heat is influenced by the recycling history of the scrap raw material used. The resulting anisotropy has led to laps and general hot rolling dysfunction due to poor distribution of especially solute precipitates.

5.1.3 Weldability

The presence of both large numbers and types of elements rather than the carbon content is also the major factor underlying in the occasionally poor response to welding in Paper 3. Over 15% of the samples examined returned weld cracks making it hard to foresee the correct response because of the unpredictably varying alloying effect of the tramp elements both from sample to sample and within the same sample. This was more notable in the case of boron content in the cracking weld sample was 0.002<B<0.004.

5.1.4 Reinforcement Value of Bars

There was a general rise of the strength beyond the nominal values and often at the expense of other reinforcement bar properties. This was a result of the elemental content distribution (Paper 4) and is likely to increase with time as more scrap is recycled in the absence of industrial processes to remove the tramp elements and control general elemental content to stricter brackets. Up to 22 percent of the recycled TMT steel sampled in the present study gave rise to above the predetermined design (nominal maximum) yield stress value of 550Mpa. This has made the bars less suitable for reinforcement both as twisted and thermo-mechanically treated bars since their development lengths keep varying from those determined during preconstruction sample tests.

5.1.5 Thermo-Mechanically Treated Bars

The fact that in one bar the hardenability value varies to the extent that the ring to core ratio of hardness varies as shown in the plots in Paper 5 shows there is serious and consequential variation in micro element distribution both across the section and along the length of the bars (Fig. 4.17 and 4.18). This is a clear indication of the low quality returned by the TMT bars as the result of the final refinement process in the ladle and the quality of the input scrap at the crucible furnace stage. Fig.4.21 and Fig. 4.22 show that the rise in yield corresponded linearly with the Boron content, an indication that in between the production process stages, the vessels contaminate the liquid metal and the boron content that results affects the thermo-mechanical treatment of the bars to the extent that they cannot be predictably relied on for effective concrete reinforcement.

5.2 Recommendations

Regarding objective 1, the min mills option based on induction furnaces is strongly recommended for recycling purposes given the fact that it has proved resilience in the national steel business environment. The introduction of DRI in the foreseeable future is a must especially as sweetener to gradually reduce the tramp element content. A larger state involvement and wider investor base would be essential in this case.

Since the observed defects in the steel bars in the investigation on objectives 2, 3, 4 and 5 have common causes; the corresponding recommendations are also common to all and are divided into various principal groups:

a) stirring the liquid metal to homogenize the casting,
b) tramp element removal and;
c) improved sorting techniques.

a) **Stirring liquid metal**

The tendency to varying composition can be reduced to a minimum if secondary refining is stressed prior to casting. The teeming ladle is used to hold steel for some time to allow the completion of the deoxidation/decarburization processes started in the melting furnace besides. homogenization of temperature. Secondary refining can be introduced at this stage and can be realized by one or a combination of some of the following technologies:

i) Vacuum treatment (degassing) in which the steel is exposed to a vacuum to promote transfer of dissolved gases from the liquid steel to gas phase by shifting the equilibrium conditions to favour the reaction between oxygen and carbon dissolved in the steel to produce carbon monoxide. It can also be carried out in order to encourage the stirring action of the carbon monoxide as it surfaces; lifting non-metallic inclusions with as it reduces the hydrogen content. It also tends to induce chemically reducing conditions in the ladle system. When this happens, the aluminium oxide refractory particles can be reduced to give dissolved aluminium in the steel.

   Though this process, the total number of inclusions per unit area (mm^2) and the inclusion size (μm) are reduced while their distribution per unit volume (mm^3) is made more uniform, encouraging the production of more constant steel values.

ii) An oxygen lancing facility consisting of a vertical water cooled lance for blowing oxygen on the molten steel surface can be attached to the ladle for final decarburization to keep the carbon content inside stricter brackets. This process not only decarburizes, but also guarantees a uniform temperature and elemental distribution and an overall constant composition of the liquid steel in the ladle.

iii) A more conventional facility is argon gas stirring. In this process, a porous plug is used to provide gas stirring of the molten metal to promote homogenization by percolating argon gas through a plug arrangement in the bottom of the ladle. Injecting inert gas into the tundish from its bottom can also improve mixing of the liquid steel and promote the collision and removal of inclusions in addition to lowering total oxygen.

iv) Facilities for electromagnetic induction stirring (EMS) reduce on the cost of argon. Here, induction stirrers are placed in the mould, below the mould and in the final solidification zone working much like induction motor stators by producing a travelling magnetic field which generates a force field in the strand. They are generally more practical although they have a limited effect on the overall crucible composition.

b) **Tramp element removal**

i) The top slag cover in the ladle and tundish insulate the molten steel both thermally and chemically absorb inclusions to provide additional steel refining. Inexpensive organic slag cover like rice husks can be used albeit their inherent contamination risk while basic CaO-Al_2O_3-SiO_2/SiO_2 based synthetic slag cover can be more reliably used for inclusion control and reduced tundish total oxygen control. Synthetic slag cover can be used to control nitrogen levels in steel by contacting liquid metal with titanium oxides-containing slag.

ii) Sodium carbonate (Na_2CO_3) addition on an industrial basis can efficiently remove Boron from liquid iron. Injection of about 100 kg sodium carbonate per ton of the molten metal would virtually remove all Boron from liquid iron.

An alternative route for the removal of Boron would be through the use of nitrogen in calculated stoichiometric ratios of 1:1. Nitrogen is added to liquid steel in the form of nitrogen-bearing alloying additions during remelting which include nitrided ferromanganese, nitrided ferrochrome, a vanadium-nitrogen compound, nitride metallic manganese and silicon nitride (Si_3N_4).

Since most of the Boron comes into steel though boric acid binder, replacing it with the alterative calcium aluminate cement would go a long way towards reduction and control on the Boron content in induction furnace made steel.

iii) The use direct reduced iron (DRI) or hard briquetted iron (HBI) pellets to dilute the effects of these residuals. In Uganda, this is particularly recommended on the strength of the recent discovery of natural gas reductant and the abundance of iron ore. The dilution value in scrap melting are meaningful after 40% DRI addition and is due to the fact that DRI inherently contains low amounts of tramp elements and sulphur. While the recent development of sponge iron production in Jinja is a step in the right direction, there is, nonetheless, need to strengthen this effort though direct state intervention and increased investor harnessing in order to support the recycling industry with virgin steel input.

c) **Improved sorting techniques**

i) Of great importance too is the sorting process prior to the melting of scrap. The employment of specialized scrap dealing and sorting would enable the quality of scrap to be classed so that upon purchase, the average composition of the scrap is known to the melter and scrap is graded to suit product requirement.

X-ray Fluorescence (XRF) analysis can be used at the scrap metal sorting stage to measure the key elements in a range of metal alloys such as stainless, tool and low alloy steels, nickel, titanium, copper, cobalt and aluminium alloys usually with hand held equipment. These tools enable the dealer to group scrap types in accordance to their elemental composition.

5.3 Recommendation for Further Research

This research has largely achieved its objectives in examining the reliability of steel made from recycled scrap in Uganda.

An extensive study of the mechanical and chemical qualities of the steel was also done and Paper 2 was written and disseminated at the ASME conference 2012. The capacity of the steel bars to satisfy structural needs through welding, the building requirements though strength and ductility values was also examined through two papers and finally the effectiveness of the thermo-mechanically treated bars was studied and the results disseminated in the publication of Paper 5.

The poor state of homogeneity of the steel and therefore the difficulty in prediction the composition and properties together with the importance of furnace lining in the introduction of boron into the steel are important details in the findings in this research.

An overall increase in tramp element content in the Ugandan recycled steel is predictable given the reducing quality and quantity of scrap on the market unless measures are taken to introduce diluents through the use of virgin ore. The exploitation of virgin ore in the western part of Uganda and the use of sponge iron (DRI) in Jinja based factories is the most relevant and lasting step in the improvement of the overall quality of recycled steel in the country and would lead to the reduction of the tramp element content in the cycle over the years.

More research openings have, however been seen in the course of the research. More ample identification of the effect of individual elements in the quality of the steel in the country is needed in addition to what has been done in the present research; the salient nature of elements like Boron was highlighted. Further research could be used to quantify the effect of these elements more precisely. A study of the position of these elements and the identification of solutions aimed at the regulation of the identified and quantified elements in an absolute research necessity.

The significance of the fracture forms of the steel bars is also an open and much needed area of research since a lot can be deciphered about the state of the metal from documented characteristic fracture modes.

Research on the economic significance of steel recycling in Uganda is an area of interest for additional research.

REFERENCES

ACI 318-08, 2008. Building Code Requirements for Structural Concrete and Commentary. Reported by ACI Committee 318, American Concrete Institute, Farmington Hills, MI, 465 p.

Arabinda S., Bidyapati S., 2011. Sponge Iron Production in Rotary Kiln

Antonio A, 2009. Steel Forming and Heat Treating Handbook, São Vicente, Brazil.

ARC (Australian Reinforcing Company), 2008. Reinforcement Handbook: Guide to Steel Reinforcement.

Atkinson H. and Shi G. 2002. Characterization of Inclusions in Clean Steels: A Review Including the Statistics of Extremes Methods, Department of Engineering Materials, University of Sheffield, Mappin Street, Sheffield, UK.

Avramovic C., Ososkov M., Jain, Wilkinson, (2008). Effect of Martensite Distribution on Damage Behaviour in DP600 Dual Phase Steels, Materials Science and Engineering a doi:10.1016/j.msea.2009.03.055

Bailey, Coe F, Hart, Gooch, 2004. Welding steels without hydrogen cracking. $2^{nd.}$ Ed. Woodhead Publishing Ltd.

Beno S and Larso D., 2013. Proposal on Electric Arc Furnace Utilization to Achieve Cost Optimization. The Indonesian Journal of Business Administration Vol. 2, No. 15, 2013:1791-1801

Bhupinder S. and Kaushik S, 2002. Influence of steel-making processes on the quality of reinforcement. The Indian Concrete Journal.

BIR (Bureau of International Recycling), 2011. World Steel Recycling in Figures, Steel Scrap – a Raw Material for Steelmaking.

Brown J. 2001. Ferrous Foundry Man's Hand Book, Foseco International Ltd, 11^{th} Ed.

Buehler, Markus J. 2005. The dynamical complexity of work - hardening: a large-scale molecular dynamics simulation. Acta Mech Sinica. pg 103-111.

Caoa H., Mina J., Wua S., 2006. Pinning of Grain Boundaries by Second Phase Particles in Equal-Channel Angularly Pressed Cu–Fe–P Alloy Elsevier, Materials Science and Engineering. A 431 86–91

Carter T., Cornish, 2001. Hydrogen in Metals. Vol. 8, Issue 2, April 2001, Pages 113–121

Chatterjee A., 1995. Recent Developments in iron making and steel making. Iron and Steelmaking pp. 100-104.

Chong C., 2008. Effect of Alloying Elements on Steels, Inspector Knowledge Series 04-0 pp. 49**.**

Christian B., 2007. Effective use of residual elements in steels produced from scrap. Swedish Institute for Metals Research, D 822 KIMAB 367023

Cogne J, Heritier B, and Monnot J., 1987, Clean Steel, Institute of Metals, London, pp. 29–31

Daramola, Adewuyi and Oladele, 2010. Effects of Heat Treatment on the Mechanical Properties of Rolled Medium Carbon Steel. Journal of Minerals & Materials Characterization and Engineering, Vol. 9, No.8, pp.693-708.

Devletian J. and Van D., 2008. Failure Analysis of Steel Welds. ASM International, DOI:10.1361/faht2008, pp 503-519.

Dutta S., Lele A. and Pancholi N.(2004). Studies on Direct Reduced Iron Melting in Induction Furnace, Trans. Indian Inst. Met., Vol. 57, No. 5.

EAS 412-2005. East African standard: Steel for the reinforcement of concrete.

Fang C., Lundgren K., Chen L. and Zhu C 2004, 'Corrosion influence on bond in reinforced concrete', Cement and Concrete Research, vol. 34, no. 11, pp. 2159–2167.

Fujda M., 2003**.** Effect of Copper Content on the Hot Ductility Loss of Low Carbon Steels. Journal of Metals, Materials and Minerals. Vol. 12 No. 2 pp. 27-31.

Garza L. and Van T., 2005. Surface Hot-Shortness of 1045 Forging Steel with Residual Copper. Journal of Materials Processing Technology 159, pp. 169-180.

Grange, R., Hribal, C., Porter, L., 1977. Hardness of Tempered Martensite in Carbon and Low Alloy Steels. Metallurgical Transactions A, Vol. 8, Issue 11, pp.1775-1785.

Gregg B., William K., Neely J. and Kibbe R., (2004). Modern Materials and Manufacturing Processes, 3/E, ISBN-10: 0130946982 • ISBN-13: 9780130946980.

Grigorovich K., Shibaev S., and Kostenko I., 2010. Ferroalloys for Clean Steels Production and Quality Specifications. The Twelfth International Ferroalloys Congress, Helsinki, Finland.

Grobler F. and Minnitt R., 1999. The increasing role of direct reduced iron in global steelmaking. The Journal of the South African Institute of Mining and Metallurgy.

Haley G., 2012. Nitrogen Levels in Ductile Iron. The 2002 Ductile Iron Society Annual Meeting Pioneer Resort and Marina; Oshkosh, Wisconsin.

Herman J., Leroy V., 1996. Influence of Residual Elements on Steel Processing and Mechanical Properties C.R.M. rue Ernest Solvay 11, 4000 Liège, Belgium Presented at "Metal Working and Steel Processing" Cleveland, October 14-17, 1996

Honeycombe R., Bhadeshia H., 2006: Steels: Microstructure and Properties, Third Edition Elsevier Science and Tech, Technology and Engineering.

Ibrahim H., 2010. Steel Raw Materials In Nigeria Raw Materials Research and Development Council 17, Aguiyi Ironsi Street, Maitama District, Nigeria

Islam M., 2010. Thermo-mechanically Treated Advanced Steels for Structural Applications Proceedings of MARTEC 2010, 11-12 December 2010, BUET, Dhaka, Bangladesh.

Ismaeel A, Haido H., 2013. Bond Strength of Concrete with the Reinforcement Bars Polluted with Oil European Scientific Journal, vol.9, No.6 ISSN: 1857 – 7881 (Print) e - ISSN 1857-7431.

Jenkins L., 2001. The Effect of Boron in Ductile Iron. Ductile Iron News Strongsville, Ohio, USA Issue 1, 2001.

Jung , 2005. Technical efficiency of the iron and steel industry: A Stochastic frontier approach.

Janke D., Savov L., Weddige H.J., E. Schulz (2000). Scrap-Based Steel Production and Recycling of Steel. Freiberg University of Mining and Technology.

Jubleanu A., 2009. Carbo-Nitride Precipitation and Its Effects on Matrix Transformations in High-Strength / High-Toughness 300m Steel. Department of Metallurgy and Materials, University of Birmingham.

Kakani S. and Kakani A, 2006. Material Science. A New Age International Publishers, 1st Ed. pp 213.

Krauss G. (2003). Solidification, Segregation, and Banding in Carbon and Alloy Steels, Metallurgical and Materials Transactions, B 792—Volume 34b.

Krishna L., 2007. Principles of Engineering Metallurgy New Age International Publishers.

Lifeng Z., Brian G. Thomas, 2003. Inclusions in Continuous Casting of Steel. XXIV National Steelmaking Symposium, Morelia, Mich, Mexico, 26-28, pp. 138-183.

Madar D., 2009. Big SteelTechnology, Trade, and Survivalin a Global Market, ABC Press, Vancouver, Canada.

Markan K., 2004. Relevance of Quenching and Tempering Technology to India, Economic Research India Ltd.

Mehran M., 2007. The Effects of Alloying Elements on Steels, Christian Doppler Laboratory.

Melford D.1980. The Influence of Residual and Trace Elements on Hot Shortness and High Temperature Embrittlement. The royal society.

Meyers, Marc, Chawla, Krishan, 2009. Mechanical Behavior of Materials (2ndEd.) Cambridge University Press pg 420-425.

Mongkol J., 2008**.** Reinforced Concrete Design, Bond, Anchorage, and Development Lengths.

Monideepa M., Chaitali D., Arunansu H., 2012. Prediction of Hardness of the Tempered Martensitic Rim of TMT Rebars. Research and Development, Tata steel, Jamshedpur, 831001, India.

Mukhopadhyay A., Galasso L., 2011. Better Control for Mechanical Properties of Quenched and Tempered Bars, Tecnol. Metal. Mater. Miner., São Paulo, v. 8, n. 4, pp. 230-236.

Murali F., Roberto R. (2011), Effect of Boron on microstructure and mechanical properties of multiphase steel.

Naro, 2004. Elimination and Neutralization of Boron in Ductile Irons ASI International, Ltd., Cleveland, Ohio.

Nawy E, 2004. Reinforced concrete: a fundamental approach, University of Maryland, College Park.

Newby J, Mills K. (1989) Metals handbook: Metallography and Microstructures. 9th ed. ASM International.

Nibinfo, 1998, (Niobium Information 17/98). Characteristic fatures of Titanium, Vanadium and Niobium as Micro Alloy Additions in Steel.

Nordstrand F., 2009. The Metallurgical Foundation for Manufacturing of CeS-Based Grain Refiners for Steels.

Nylén T; 1982. Influence of Cu, Sn and other residuals on the break-out frequency and amount of surface defects during continuous casting. Stockholm; Sweden: IM report 1763.

O'Neill D., 2002: An investigation of surface hot shortness in low carbon steel. University of New South Wales, Australia.

Olivier R., Christian B. and Margareta N., (2006), Opportunities and Dangers of Using Residual Elements in Steels: A Literature Survey: KIMAB.

Othani H, Suda H, Ishida K. (1997). Solid/Liquid Equilibria in Fe-Cu based ternary systems. Addis Ababa; Ethiopia: ISIJ International, vol.37, No.3, pp.207-216.

Pirowski Z., Wodnicki J., Olszyński J. 2007. Micro-additions of Boron and Vanadium in ADI, Part 1. Literature review. Archives of Foundry Engineering, Vol.7, Issue 1/2007, 167-170.

Poursaeidi E., 2008. The Causes of Local Hardness Increasing in Power-plant Rotors and its Modification by Tempering.

Prabir C., Shylamoni P., Roshan A. 2004. Characterization of steel reinforcement for RC structures: An overview and related issues. The Indian Concrete Journal,.

Raghavan V., 2004. Materials Science and Engineering: A First Course. Eastern Economy Edition. 5th Ed. pp264

Satish V., 2009, Materials Science. Dept. of Mech. Eng., Indian Inst. of Science, Bangalore – 560012, India, Ch. 7.

Savov L., Elena V, Dieter J., 2003. Copper and Tin in Steel Scrap Recycling. RMZ Material and Geoenvironment Vol.50 N0.3, pp637-640.

Senfuka C, Kirabira J., Byaruhanga J., 2011. Options for Improvement of the Ugandan Iron and Steel Industry. Proceedings of the Second Interentionl Conference on Advances in Engineering and Tenchnology, Entebbe, Uganda, Jan. 31st –Feb.1st 2011; 1AET2011 (013).

Senfuka C, Kirabira J.B, Byaruhanga J., 2012. A Quantitative Evaluation of the Quality of Recycled Steel in Uganda; Proceedings of the ASME November 9-15, 2012, Houston, Texas, USAIMECE2012-85276 congress).

Smith W., Hashemi J., 2006. Foundations of Materials Science and Engineering, 4th Edition, McGraw-Hill College, ISBN 0-07-295358-6, pp 243.

Spies, H.J., 1992. Mechanical properties of ferrous and nonferrous alloys after quenching, Theory and technology of quenching, Liščić, B., Tensi, H., Luty, W. (eds.), Springer-Verlag, Berlin.

Suksai S., 2007. Mechanical Design Handbook: Hardness and hardenability of materials AISI 415 - UNS S 41500 Bleche und Zuschnitte, pp.237.

Tamm F. and Markan R. 2010. Technology for High Strength Rebars-The Process and Results, CMD. H&K India.

Thompson S. and Howell P.R, 1992. Materials Science Technology, vol. 8, pp. 777-84.

Tian Gao and Cristopher D., 2010. The Cold Work of Forming Effect in Steel Structural Members, Dept. of Civil and Environment Eng., Virginia Tech.

Tupkary R.H and Tupkary V.R., 2008. An Introduction to Modern Steel Making. Khanna Publishers, Delhi-110006.

UBOS (Uganda Bureau of Statistics), 2009, Statistical Abstract.

Uchino H, 2001. Effects of C and P on Surface Hot Shortness of Steel Due to Cu Mixed from Steel Scrap', Univ. Tokyo, Tokyo, Japan.

URA, 2010 (Uganda Revenue Authority), Iron and Steel, Pge.1, October, 2010.

Valipour M., 2009. Mathematical Modeling of a Non-Catalytic Gas Solid Reaction: Hematite Pellet Reduction with Syngas Transactions C: Chemistry and Chemical Engineering Vol. 16, No. 2, pp. 108-124

Vogel M., Janke D. and Savov L., 2006. Secondary Materials in Steel Production and Recycling. Institute of Iron and Steel Technology, TU Freiberg, Springer. Printed in the Netherlands.

Wang S., Peng Y. and, Li Z., 2013. Work-Hardening and Deformation Mechanism of Cold Rolled Low Carbon Steel Research Journal of Applied Sciences, Engineering and Technology 5(3): 823-828, ISSN: 2040-7459; E-ISSN: 2040-7467

Wencora M, Takahashib A, Ghoniema N., 2005. Kinetics of Self-Interstitial Cluster Aggregation near Dislocations and their Influence on Hardening.

Wolfgang R. Schütze, 2006. Hot Briquetting of Direct Reduced Iron; Technology and Status of Industrial Applications, D-45529 Hattingen/Ruhr, Germany.

Xu Youlin, 2010. Optimization and Selection of Reinforced Steel Bar Applicable in the Code for Concrete Structures of P. R. China; China Academy of Building Research.

Yamamoto K, Shibata H, Mizoguchi S., 2005, ‘Defective or effective? – tramp elements in steel’, Trans, Indian Inst. Met. Vol.58, No.4, pp. 695-702.

Yousef P. and Mansour S., 2007. Oxide Inclusions at Different Steps of Steel Production, Journal of Iron and Steel Research, International.

Yu Jin J. and Sang W., 2007. An Estimation of a Billet Temperature during Reheating Furnace Operation: International Journal of Control, Automation, and Systems, vol. 5, no. 1, pp. 43-50.

Yuan Z., Jia J., Guo A., Shen D., Song S, Liu J. (2003). Influence of tin on the hot ductility of a low-carbon steel. Milan; Italy: Acta Metallurgica Sinica, vol.16, no.6, pp.478-482

Yurioka N., Okumura M., Kasuya T., Ohshita S., 1985. Welding Note, 3rd ed., Nippon Steel, Japan pp.48-50. Modern Materials and Manufacturing Processes, 3/E

APPENDICES

APPENDIX 1, Paper 1: Options for Improvement of the Ugandan Iron and Steel Industry.

APPENDIX 2, Paper 2: A Quantitative Evaluation of the Quality of Recycled Steel.

APPENDIX 3, Paper 3: The Concrete Reinforcing Value of Recycled Steel Bars.

APPENDIX 4, Paper 4: Weldability of Recycled Steel Bars in Uganda.

APPENDIX 5, Paper 5: Thermo-Mechanically Treated Bars Made from Recycled Steel.